RANK 1 FIRST FORBIDDEN BETA-DECAY LOG(FT) VALUES FOR SOME GOLD ISOTOPES

2022
MASTER THESIS
PHYSICS

Mohammed Hawez SABER

Thesis Advisor
Prof. Dr. Necla ÇAKMAK

RANK 1 FIRST FORBIDDEN BETA-DECAY LOG(FT) VALUES FOR SOME GOLD ISOTOPES

Mohammed Hawez SABER

T.C.
Karabuk University
Institute of Graduate Programs
Department of Physics
Prepared as
Master Thesis

Thesis Advisor
Prof. Dr. Necla ÇAKMAK

KARABUK
January 2022

I certify that in my opinion, the thesis submitted by Mohammed Hawez SABER titled "RANK 1 FIRST FORBIDDEN BETA-DECAY LOG(FT) VALUES FOR SOME GOLD ISOTOPES" is fully adequate in scope and quality as a thesis for the degree of Master of Science.

Prof. Dr. Necla ÇAKMAK .....
Thesis Advisor, Department of Physics

This thesis is accepted by the examining committee with a unanimous vote in the Department of Physics as a Master of Science thesis. Jan 14, 2022

Examining Committee Members (Institutions)	Signature
Chairman : Prof. Dr. Necla ÇAKMAK (KBU)	.....
Member : Assist. Prof. Dr. Ahmet Mustafa ERER (KBU)	.....
Member : Assist. Prof. Dr. Şadiye ÇAKMAK (ESOGÜ)	.....

The degree of Master of Science by the thesis submitted is approved by the Administrative Board of the Institute of Graduate Programs, Karabuk University.

Prof. Dr. Hasan SOLMAZ .....
Director of the Institute of Graduate Programs

"I declare that all the information within this thesis has been gathered and presented in accordance with academic regulations and ethical principles and I have according to the requirements of these regulations and principles cited all those which do not originate in this work as well."

Mohammed Hawez SABER

ABSTRACT

M. Sc. Thesis

RANK 1 FIRST FORBIDDEN BETA-DECAY LOG(FT) VALUES FOR SOME GOLD ISOTOPES

Mohammed Hawez SABER

Karabük University
Institute of Graduate Programs
The Department of Physics

Thesis Advisor:
Prof. Dr. Necla ÇAKMAK
January 2022, 58 pages

The log(*ft*) values of the rank1 first forbidden (FF) transitions were investigated by using Schematic Model (SM) for even-even neutron-rich isotopes of Gold (Au). We solved only in the particle-hole channel the secular equations of the rank1 transitions the eigenvalues and eigenfunctions of the Hamiltonian within the framework of proton-neutron Quasi Random Phase Approximation (pn-QRPA). The Woods-Saxon (WS) potential basis was used in our calculations. The relativistic beta moment matrix element of the rank1 transition was calculated directly without any assumption. In all calculations, each Au nuclei was considered in a spherical shape. The calculated log(*ft*) values of the rank1 first forbidden transition compared with the experimental studies and the obtained results were found to be closer to these values.

Keywords **:** rank1 transition, pn-QRPA, Woods-Saxon potential, Schematic Model

Science Code : 20216

ÖZET

Yüksek Lisans Tezi

BAZI ALTIN İZOTOPLARININ RANK 1 BİRİNCİ YASAKLI BETA-GEÇİŞ LOG(FT) DEĞERLERİ

Mohammed Hawez SABER

Karabük Üniversitesi
Lisansüstü Eğitim Enstitüsü
Fizik Anabilim Dalı

Tez Danışmanı:
Prof. Dr. Necla ÇAKMAK
Ocak 2022, 58 sayfa

Çift-çift nötron zengini altın (Au) izotoplarının rank1 birinci yasaklı geçişlerinin log(*ft*) değerleri şematik model (SM) kullanılarak incelendi. pn-QRPA çerçevesinde Hamiltonyenin özdeğerleri ve özfonksiyonları rank1 geçişlerinin seküler denklemleri için sadece parçacık-boşluk kanalında çözüldü. Hesaplamalarımızda Woods-Saxon (WS) potansiyeli kullanıldı. Rank1 geçişinin rölativistik beta moment matris elemanı herhangi bir yaklaşım yapılmaksızın doğrudan hesaplandı. Bütün hesaplamalarda her bir Au çekirdeği küresel formda kabul edildi. Rank1 birinci yasaklı beta geçişlerinin hesaplanan log(*ft*) değerleri deneysel çalışmalar ile karşılaştırıldı ve elde edilen sonuçlar bu değerlere yakın olarak bulundu.

Anahtar Kelimeler : rank1 geçişleri, pn-QRPA, Woods-Saxon Potansiyeli, Şematik Model

Bilim Kodu : 20216

ACKNOWLEDGMENT

I would like to thank my advisor, the head of the Physics Department, and the head of the Nuclear Structure Theory group, Prof. Dr. Necla ÇAKMAK. She was always ready for my questions and problems and created a nice atmosphere to work in.

Special thanks go to my wife and my children, for supporting me during this thesis.

CONTENTS

Page

LIST OF FIGURES

Page

LIST OF TABLES

Page

SYMBOLS AND ABBREVIATIONS INDEX

SYMBOLS

Au	: Gold
A	: Mass number
Z	: Protons number (number of nuclear charges)
N	: Neutrons number
e^-	: Electron
c	: Speed of light
e^+	: Positron
g_V	: Vector interaction constant
g_A	: Axial vector interaction constant
$t_-(k)$	: Isospin decrease reduction operator
r_k	: Radius vector of the nucleon
$\vec{Y}$	: Spherical harmonic operator
$C_{jmc\gamma}^{j'm'}$	: Clebsch-Gordan coefficient
$\vec{\nabla}$	: Nabla operator
$\vec{\sigma}$	: Pauli spin operator
$\hat{I}$	: Unit operator
χ_{ph}	: Particle-hole effective interaction constant
J^π	: Spin–parity
j_A	: Axial vector flux
$\hbar$	: Plank constant
ft	: Decay time

ABBREVIATIONS

β	: Beta transition
GT	: Gamow-Teller decay
F	: Fermi transition
FF	: First forbidden transitions
FFR	: First forbidden resonance
2νββ	: Double beta decay
RPA	: Random phase approximation
QRPA	: Quasi-particle random phase approximation
pn-QRPA	: Proton-neutron quasi-particle random phase approximation
pn-RQRPA	: Renormalized proton-neutron quasi-particle random phase approximation
WS	: Woods-Saxon potential
PM	: Pyatov method
SM	: Schematic model
IBM	: Interacting boson model
sp	: Single-particle
qp	: Quasi-particle
ph	: Particle-hole
pp	: Particle-particle
$\widehat{H}_{op}$	: Hamilton operator (weak interaction Hamilton)
$\widehat{H}_{sqp}$	: Single quasi-particle Hamiltonian operator
Q	: Decay energy
pn-QTDA	: Proton-neutron quasi-particle Tamm–Dancoff approximation
EC	: Electron capture
ECC	: Electron capture cross-section
EOM	: Equations of motion
BCS	: Bardeen–Cooper–Schrieffer theory
R_{np}	: Radial neutron-proton integral

β^- : Negative beta decay (negatron capture)

β^+ : Positive beta decay (positron capture)

ε : Single particle energy

$\bar{\nu}_e$: Antineutrino

m_n : Mass of the neutron

m_p : Mass of the proton

m_e : Mass of the electron

ν_e : Neutrino

m_{e^+} : Positron mass

ψ_i : Initial wave function

ψ_f : Final wave function

G_F : Fermi constant

λ : Decay rate

$\rho(E_f)$: Final state density

M_{fi} : Final and initial nuclear matrix element

E_f : Final state energy

E_e : Electron energy is constant

J : Angular momentum

π : Parity

V_C : Coulomb potential

V_{central} : Central potential

$V_{so}(\vec{l}, \vec{s})$: Spin-orbit potential

CS : Condon-shortley phase layout

BR : Biedenharn-rose phase layout

QBA : Quasi-boson approximation

ω_i : Ground state energy of the neighbouring nucleus

PART 1

INTRODUCTION

The beta-decay process is a radioactivity process to understand the weak processes of the interacting and nuclear structure. Although literature scientists have conducted many theoretical and experimental studies on allowed transitions, they did not show the same importance in forbidden transitions. Recent research has shown that the first-forbidden (FF) of the beta transition process is useful in determining the correctness theories relating to the r-processes and $2\nu\beta\beta$ [1].

In 1950, experimental and theoretical studies began on the first-forbidden (FF) beta transitions, and a general theory was created in 1951 about the first-forbidden (FF) beta-decay [2].

In addition, factors such as half-lives and beta-decay properties play a role in selecting the observed abundances in exotic nuclei near the path [3]. Due to the inaccessibility of many r-process progenitors with current radioactive ion beam facilities, estimates of r-process nucleosynthesis typically rely on predictions based on nuclear models describing properties of nuclei that are far from stable [4]. On the other hand, for extreme isospin values, microscopic structural effects altering the shape of the β-strength function, such as quenching or distortion of nuclear shells, can bias theoretical predictions [5,6].

Not only does electron neutrino capturing intensify the impact of beta-decays in neutron-rich environments, but neutron spallation induced by electron neutrinos may also play a role in modifying r-abundance distribution [7].

The ground state transitions in first-forbidden (FF) and allowed Gamow-Teller (GT) beta-decays are studied by Suhonen [8]. The unique first-forbidden (U1F) for J =2 is calculated and the Gamow-Teller (GT) transitions are allowed in even-even and odd-

odd nuclei in the mass range $70 \leq A \leq 214$ [9]. It is proposed that at ^{200}Au decay, a level of ^{200} Hg at 2,642 kV is populated by the main beta-decay branch [10]. Halbleib and Sorensen developed the quasi-particle random phase approximation (QRPA) model by generalizing the ordinary random phase approximation (RPA) to depict charge-exchanging transitions [11]. Proton-neutron quasi-particle random phase approximation (pn-QRPA) uses pairing interaction to construct a quasi-particle basis, and the random phase approximation (RPA) equation is used to calculate the schematic first-forbidden (FF) residual interaction. To study the first-forbidden (FF) transitions with a schematic disjoin interaction, the proton-neutron quasi-particle random phase approximation (pn-QRPA) model is analyzed using the Woods-Saxon (WS) potential basis in the Chepurnov parameterization [1].

Civitarese et al. presented the factor of spin-isospin dependent interactions on first-forbidden (FF) β-transitions of low-energy between even-odd and even-even nuclei with $\Delta J = 0, 2$. The relativistic beta momentum matrix element $M^{\pm}(\rho_A, \lambda = 0)$ is not analytically evaluated; the non-relativistic beta momentum matrix element $iM^{\pm}(j_A, k = 1, \lambda = 0)$ is assumed to be proportional. The *ft* values were calculated for the ground state for $\Delta J = 0,2$, and it was shown that the first-forbidden (FF) beta decay giant resonances occurred at approximately 25 MeV. Charge change spin-dipole calculations include the effect of nuclei polarization [12].

Kenar İ., et al. presented nuclear matrix elements that were calculated for rank 0 transitions without considering the communion from spin-orbit potential in the evaluation of the relativistic matrix element. The $0^+ \rightarrow 0^-$ first-forbidden (FF) beta-decay was examined for $^{206\text{-}2014}Pb \rightarrow ^{206\text{-}2014}Bi$ transitions and the calculations were made according to two different approaches [13,14]. For the first approximation, the relativistic beta transition operator is evaluated straight away without making any assumptions. The second approximation considers the relativistic operator as proportional to the non-relativistic operator. The first-forbidden (FF) beta-decay matrix element has been computed without taking into account spin-orbit interaction in the shell model potential. In comparison to other studies, the results obtained are closer to the experimental data, although it cannot be said that they are in complete harmony. The reason for this is that in these calculations, the effective interaction

with charge change between nucleons is only considered in the particle-hole (ph) channel. The interaction in the particle-particle (pp) channel is very important for a better understanding of the weak interaction theory. 0^- excited states were examined for spherical nuclei. The contribution from the spin-orbit potential is considered in the evaluation of the relativistic matrix element of the first-forbidden (FF) beta transition matrix element, which is evaluated without any assumptions. Particle-particle (pp) and particle-hole (ph) spaces are based on calculations [15]. Using the ξ- approximation, log*ft* values for ^{124}Sb and ^{86}Rb for the first-forbidden (FF) beta-decay [16] and single-particle (sp) log*ft* values for ^{207}Ti→ ^{207}Pb and ^{209}Pb→ ^{209}Bi transitions using the same approach [17].

Nabi, J., et al. presented the properties of β-decay of the nucleus with some neutron N= 126. Two various factors of the proton-neutron quasi-particle random phase approximation (pn-QRPA) model were utilized to evaluate half-lives and the β-decay rates for N = 126 isotones. The schematic model (SM) approach is used to analyze and calculation the proton-neutron quasi-particle random phase approximation (pn-QRPA) equations. As an average field base, the Woods-Saxon (WS) potential was used. Both first-forbidden (FF) and allowed Gamow-Teller (GT) transitions were considered in the particle-hole (ph) channel. Under stellar and terrestrial settings, the proton-neutron quasi-particle random phase approximation (pn-QRPA) model was used in the distorted Nilsson basis to evaluate the β-decay rates for unique first-forbidden (U1F) and allowed Gamow-Teller (GT) transitions. The findings support the results of the shell model, showing that first-forbidden (FF) transitions because of a significant change in the isotones' evaluated half-lives. The use of first-forbidden (FF) communion resulted in a substantially greater agreement between evaluated and measured terrestrial-decay half-lives than previous computations. An example of waiting point nuclei's influence on the r-process nucleosynthesis is given [18].

Nabi, J., et al. presented increasing proton number (Z) causes to show more importance first-forbidden (FF) charge-changing transitions for nuclei, and this is because of decreasing of the allowed Gamow–Teller (GT) strength transitions. They calculated allowed Gamow–Teller (GT) also $0^+ \rightarrow 2^-$ and $0^+ \rightarrow 0^-$ transitions for neutron-rich Ge and Zn isotopes. To calculate first-forbidden (FF) and allowed

Gamow–Teller (GT) transitions, two various proton-neutrons quasi-particle random phase approximation (pn-QRPA) models were combined with the interaction of a schematic separable. First-forbidden (FF) decay plays a significant role in the pn-QRPA(N) computation that includes distortion. For Zn isotopes, the pn-QRPA(WS) results are better than observed data (upper panel), although the pn-QRPA(N) results show the best overall agreement with experimental data. In order to evaluate β-stellar decay rates for astrophysical purposes, allowed Gamow–Teller (GT) and unique first-forbidden (U1F) transitions were included. ^{86,88}Ge has a significant communion to the overall stellar rate of unique first-forbidden (U1F) transitions [19].

Nabi, J. U., et al. presented first-forbidden (FF) transitions can play a significant role in reducing the evaluated half-lives especially in environments where allowed Gamow-Teller (GT) transitions are not preferred. Particularly noteworthy is phase-space amplification in neutron-rich nuclei, which favours the first-forbidden (FF) transition. They calculated the allowed Gamow-Teller (GT) transitions for nickel's even-even neutron-rich isotopes using various proton-neutron quasi-particle random phase approximation (pn-QRPA) models. The factor of distortion on the evaluated strengths of Gamow-Teller (GT) is studied. The first-forbidden (FF) transitions for isotopes of nickel even-even if they are neutron-rich are evaluated assuming that the nuclei are spherical. They took into account the distortion of the nuclei and calculated the allowed Gamow-Teller (GT) + unique first-forbidden (FF) transitions, stellar beta-decay rates, the probability of β-delayed neutron emissions, and the energy rate of β-delayed neutrons. The computed half-lives are very similar to those measured and prove that they are responsible for speeding up r-mater flow [20].

Nabi, J. U., et al. presented the allowed Gamow–Teller (GT) transitions are the majority common spin–isospin ($\sigma\tau$) type weak nuclear processes. In the field of nuclear physics, these transitions play a significant role in a variety of processes. Their communion to astrophysics, supernova explosions and particularly nuclear synthesis is very significant. First-forbidden (FF) transitions are more important when allowed Gamow–Teller (GT) transitions are disfavored, especially in heavy and medium nuclei. First-forbidden (FF) transitions are favoured in neutron-rich nuclei because of phase-space multiplication for these transitions. They determined

the allowed Gamow–Teller (GT) and the strength of unique first-forbidden (U1F) |J| =2 transitions in even-even and odd–odd nuclei in the mass range 70 ≤A≤ 214. Two different proton-neutron quasi-particle random phase approximation (pn-QRPA) models with a schematic separable interaction were used to calculate unique first-forbidden (U1F) and Gamow-Teller (GT) transitions. The inclusion of the strength of unique first-forbidden (U1F) to both models improved the total comparison of computed half-lives of terrestrial β-decay. For the $2^- \leftrightarrow 0^+$ transitions, the *ft* values and decreased transition probabilities were also determined. The rates of $\beta^{\pm}$-decay and electron/ positron capture of heavy nuclei in the stellar matter were investigated, and it was also shown that at high stellar temperatures, electron and positron capture rates control the overall weak rates of all these heavy nuclei [9].

Cakmak, N., et al. presented in open-shell ^{124,126,128,130}Te isotopes, the structure of 1^- excitations. A translational and Galilean invariant model is used to investigate electric dipole states. The same isotopes are also explained theoretically by spin-dipole 1^- excitations that conserve charge. Both types of excitations have the energy spectra analyzed and discussed. The calculated cross-sections and energy are also compared to the experimental data [21].

Ullah, A., et al. presented the role of the distortion parameter (β) on the computed strength of Gamow-Teller (GT) distributions and electron capture cross-sections (ECC) for ^{46,48,50}Cr isotopes through the framework of the proton-neutron quasi-particle random phase approximation (pn-QRPA). In this investigation, three various parameters were used. The interacting boson model (IBM) and the macroscopic-microscopic (Mac-mic) models were used to calculate two of them. The experimental values determined by using its relation with the experimental B(E2)↑ values are the third. All of the daughter states of the indicated isotopes have widely dispersed Gamow-Teller (GT) strength distributions. They were determined to have an inverse relationship with the β parameter, i.e., they decreased as the β value increased. The electron capture cross-sections (ECC) were evaluated as a function of the β parameter, and the findings show that for the selected examples, the evaluated electron capture cross-sections (ECC) decreased as the parameter β value decreased [22].

Çakmak, Ş., et al. simulated the Gamow-Teller (GT), allowed Fermi (F), and first-forbidden (FF) transitions for even-even neutron-rich zinc isotopes using the Pyatov Method (PM) and Schematic Model (SM). The Fermi beta-decay calculations were performed by using the proton-neutron quasi-particle random phase approximation (pn-QRPA) in the Pyatov method (PM) without adding the effective coupling constant values. Schematic Model (SM) and Pyatov Method (PM) were used to calculate Gamow-Teller (GT) transitions for the particle-particle (pp) and particle-hole (ph) channels using proton-neutron quasi-particle random phase approximation (pn-QRPA). In the computations for first-forbidden (FF) transitions, only the relevant particle-hole (ph) channel in the Schematic Model (SM) was taken into account. For eigenfunctions and eigenvalues of relevant Hamiltonians, they computed the secular equations of Fermi (F), Gamow-Teller (GT) and first-forbidden (FF) transitions. In all simulations, each Zn nuclei was given a spherical shape. In Schematic Model (SM) and Pyatov Method (PM) simulations, the experimental values were found to be closer to the calculated log*ft* values of the Gamow-Teller (GT) and allowed Fermi (F) transitions. It is excellent agreement the experimental equivalents of first-forbidden (FF) excitations with the simulated half-lives developed in this study, which are similar to log*ft* values [23].

One of the main problems in nuclear structure analysis and testing nuclear models is the calculation of the nuclear matrix element. As it is known, beta-decay processes are very important in understanding the nuclear structure and weak interaction processes. Especially in the nucleosynthesis event, the effect of the first-forbidden (FF) passes has gained great importance in recent years. In this thesis; for spherical nuclei in the $186 \leqslant A \leqslant 202$ mass region for Gold (Au) isotopes, the log*ft* values will be obtained by calculating the nuclear matrix elements of the first-forbidden (FF) rank1 beta transitions and important contributions to the literature will be presented.

We can list the basic features that distinguish the analytical calculations made within the scope of the thesis from other studies in the literature as follows:

- Direct calculation of beta momentum, which is relativistic from the first-forbidden (FF) beta transition momentum, without any assumptions.
- The use of the base functions of the Woods-Saxon (WS) potential as the potential well in the microscopic model is considered, since the charge and mass distribution in the nucleus in electron and proton scattering is closer to the Woods-Saxon (WS) potential function.
- Considering the interaction forces in the particle-particle channel to the effective interaction with charge change between nucleons.

The thesis study consists of:

- The relativistic and non-relativistic nuclear matrix elements of the first-forbidden (FF) $\Delta J = 1$ $\beta^{\pm}$ decay transition operators will be calculated.
- The calculation of the first-forbidden (FF) $\beta^{\pm}$ transitions will be done using the proton-neutron quasi-random phase approximation (pn-QRPA) and the particle and quasi-particle (qp) space will be taken as the basis.
- By drawing wave functions in the radial integrals of matrix elements of each case, the dependence of the radial integrals of these matrix elements to the parameters of the Woods-Saxon (WS) potential will be examined.
- The first-forbidden resonance (FFR) energies of the rank 1 excited state for the nucleic in the $186 \leqslant A \leqslant 202$ mass region for Gold (Au) and log*ft* values that contribute greatly to the compilation of nuclear decay information will be calculated and the thesis study will be evaluated in general by making comparisons with experimental data.

The thesis consists of six parts: In the first part; literature information about beta-decay processes and first-forbidden (FF) beta transitions is given. In the second part; the theory of beta decay, Fermi's Golden Rule, and the selection rules for beta decay. In the third part, relativistic and non-relativistic matrix elements of rank 1 first-forbidden (FF) β-decay transition operators were calculated. In the fourth part, the eigenvalues and eigenfunctions of the Hamilton operator were obtained only by the effective interaction of the particle-hole channel through the framework of the proton-neutron quasi-particle random phase approximation (pn-QRPA). By

considering the wave functions in the radial integrals of the matrix elements of each case, the dependence of the radial integrals of these matrix elements on the Woods-Saxon (WS) potential parameters is expressed. In the fifth part, the first-forbidden resonance (FFR) energies of the excited states of $\lambda^{\pi} = 1^{-}$ for the nuclei in the mass region for Au discussed, and log*ft* values, which contributed greatly to the compilation of nuclear decay information, were calculated and the study was generally evaluated by making comparisons with experimental data. In the sixth part, we give a summary and conclusion of the results obtained in this thesis, as well as its contributions.

PART 2

BETA-DECAY

2.1. THEORY OF BETA DECAY

The beta-decay theory was developed by Enrico Fermi in 1934 [24]. When a radioactive nucleus beta-decays, the product nucleus contains the same number of nucleons as the main nucleus. This decay process is the transformation of a neutron into a proton or a proton into a neutron. In the nucleus, there is a change in the number of protons and neutrons, but there is no change in the total number of nucleons.

One of the first radioactive events observed as a result of the nucleus emitting negative electrons is beta decay. The opposite of this, that is, the nucleus from the electrons of the atom it is possible to catch someone. Beta-decay is of great importance to understanding the nuclear structure and its weak interaction properties correctly. While nuclear beta-decay is in an isolated state between the reactions of known atomic particles, then elementary particle processes that are very closely related to beta-decay have emerged. The interaction of beta decay is expressed by a paired force smaller than electromagnetic forces, and this is called weak interaction [25]. This incident was reported by Alvarez's nuclei in 1938 released during the filling of the place where the electron of the captured atom is discharged; it could not be observed until the characteristic X-rays were found.

In 1934, Joliot-Curies first observed the emission of positive electrons (positrons) in radioactive decay. Just two years later, positron was discovered in cosmic rays. These three nuclear events are closely related and are called beta-decay. Nuclei undergo beta-decay reactions when a neutron or a proton is converted from one to the other. In a nucleus, beta-decay changes both the proton numbers (Z) and the

neutron numbers (N) by one unit: Z→Z±1, N→N ± 1 so the mass number (A = Z + N) remains constant [26]. Hence nuclear beta transitions have a very important place in understanding the weak interaction theory better, in keeping the parity, and in learning the nuclei structure with the said transitions.

The nuclear β-decay processes are defined as

$$n \rightarrow p + e^{-} + \bar{\nu}_e \qquad \beta^{-} \text{ decay} \qquad (2.1)$$

$$p \rightarrow n + e^{+} + \nu_e \qquad \beta^{+} \text{ decay} \qquad (2.2)$$

$$p + e^{-} \rightarrow n + \nu_e \qquad \text{electron capture } (\varepsilon) \qquad (2.3)$$

It is examined in three parts as [27]. A disruption in lepton number conservation leads to more exotic decay methods. For example; as in the neutrino-free double beta decay, this electron changes the number of leptons to two units [28]. Another example is electron-muon transformation, which is incompatible with lepton conservation [29]. In this study, neither the lepton breach nor the neutrino character (Majorana or Dirac) affects the results. The three processes in this study that comply with the relevant conservation laws are as follows:

2.1.1. Negative Beta Decay

This process includes two isobars when the number of nuclear charges (Z) increases by one unit, which is called nuclear β^{-} decay or negatron capture and by the reaction in equation (2.4) is expressed [30].

$$(Z, N) \xrightarrow{\beta^{-}} (Z + 1, N - 1) + e^{-} + \bar{\nu}_e \qquad (2.4)$$

where β^{-} denotes the negatron capture, N represents the neutron number; Z represents the proton number, e^{-} represents the electron and $\bar{\nu}_e$ represents the antineutrino.

Essentially, they are baryons responsible for reducing a free neutron into a free proton. In the latter case, both electrons contain leptons and antilepton. This distortion is caused by the difference in mass between a proton and a neutron. The combined decay energy, and the energy released as the final state particles' kinetic energy, is expressed by equation (2.5) in decay by negatron emission;

$$Q_{\beta^-} = m_n c^2 - m_p c^2 - m_e - c^2 > 0 \quad (2.5)$$

where $Q_{\beta^-}$is the final state of the kinetic energy of particles, m_n is the mass of the neutron, m_p is the proton mass, m_e is the electron mass and c is the speed of light [31].

2.1.2. Positive Beta Decay

If the protons number in the nucleus is high, one of the protons decomposes into a positively charged electron (positron) and a neutron. While the positron is ejected from the nucleus, the neutron remains in the nucleus. Thus, while the number of protons in the nucleus decreases, the nucleus transforms into a different atom [32]. This decay containing two isobars in which the number of nuclear charges (Z) decreases by one unit means the decay of the nucleus by the positron capture denoted by β^+ and is expressed by the reaction of equation (2.6).

$$(Z, N) \xrightarrow{\beta^+} (Z - 1, N + 1) + e^+ + \nu_e \quad (2.6)$$

where β^+ is stands for positron capture, e^+ is the positron, ν_e denotes the neutrino. The decay of a proton is accompanied by a lepton and an antilepton with a neutron, and both are accompanied by an electron. It is not allowed for a free proton to decay in this way. There is an allowed nucleus in which the excess energy required to create the proton-neutron mass difference and positron mass m_{e^+} can be used. In this case, the amount of kinetic energy (Q) is negative. The kinetic energy of particles in the final state is expressed in equation (2.7) for decay by positron capture:

$$Q_{\beta^+} = m_p c^2 - m_n c^2 - m_{e^+} + c^2 < 0 \quad (2.7)$$

where m_{e^+} is the positron mass [31].

2.1.3. Electron Capture (EC)

A process in which a proton captures an electron and converts it into a neutrino and an electron neutrino, that is, the number of nuclear charges Z decreases by one unit means electron capture (ε) and is expressed in equation (2.8).

$$(Z, N) + e^- \xrightarrow{\varepsilon} (Z - 1, N + 1) + \nu_e \quad (2.8)$$

During beta decay, electron capture can only occur when extra energy is supplied, and the kinetic energy of particles in the final state in equation (2.9) is used to express this;

$$Q_\varepsilon = m_p c^2 + m_e - m_n c^2 - c^2 < 0 \quad (2.9)$$

These processes can all occur within the nucleus multi-body environment. Particularly, the nuclear environment allows EC and β^+ processes that are impossible in free space because of Q < 0.

The total kinetic energy of leptons in the final state is used to calculate the kinetic energy (Q) of each of the processes in equations (2.5), (2.7) and (2.9). The values of the nuclei that depend on the multibody directions are related to the reflection of the mass differences.

In nuclear beta decay, the decaying nucleus feels only weak interaction at the exact moment of decay and does not interact with the remaining nucleons of the nucleus via nuclear force. Thus, the A-1 nucleon does not participate in the weak decay process. Nuclear multi-body final and initial states are the only ones with strong interactions with the other A-1 nucleon. This method is known as the impulse

approximation. Beyond the impulse approximation, the definition of beta-decay includes the processes shown in Figure (2.2.).

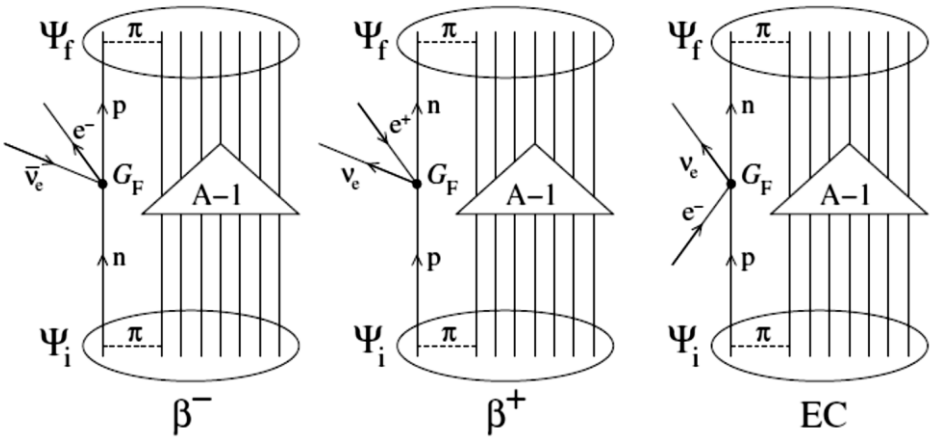

Figure 2.1. The Feynman diagrams [31].

In Figure (2.1.) it can be seen that in the impulse approximation only one nucleon participates in the weak decay process during nuclear positive beta-decay (β^+), negative beta-decay (β^-), and electron capture (EC) decays. The ψ_i initial and ψ_f end states are strong two-nucleon-interacting nuclear A-body states. The antilepton lines at the weak-interaction corners appear to move back in time. The G_F Fermi constant determines the strength of the punctate weak interaction peak.

As shown in Figure (2.1.), the flow line of nucleons corresponds to the nucleon current or weak hadronic current. Similarly, the weak leptonic current is the flow line that contains the leptons. At a weak-interaction vertex, the hadronic and leptonic currents interact. The vertex is often referred to as a pointlike in the energy range of nuclear beta-decay. The effect of exchanging the large vector bosons $W^{\pm}$ is incorporated in the Fermi-named effective decay strength constant G_F.

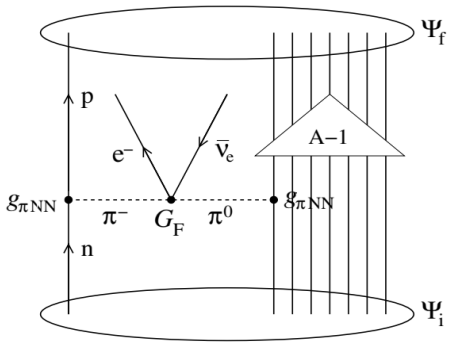

Figure 2.2. The Feynman diagram in the impulse approximation.

The weak decay of two nucleons involves an exchange of pions, as shown in Figure 2.2, with the coupling constant $g_{\pi NN}$ [31]. A closer examination of weak decay, on the other hand, reveals a more complex mechanism. It is shown in Figure (2.3) for β^- decay.

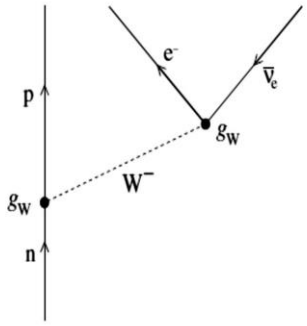

Figure 2.3. Connecting g_w with W-boson [31].

With W^- boson bonding, a neutron's binding to baryon and lepton corners through β^- decay with weakly interacting binding force g_W is shown in Figure (2.3.). The effective coupling constant G_F is due to the low energy of nuclear beta decay and the large mass of the W boson.

$$\frac{G_F}{\sqrt{2}} = \frac{g_W^2}{8(m_W c^2)^2} \tag{2.10}$$

To a good approximation, the complicated decay pattern in Figure (2.3.) can be replaced with the simple one in Figure (2.1.). The two decay lines G_F of Figure (2.3.)

are replaced by an effective vertex with an effective coupling constant G_F. A pointlike current–current interaction is described by the effective vertex [31].

2.2. FERMI'S GOLDEN RULE

In 1931, W. Pauli suggested that during the decay a second particle, which Enrico Fermi later called the neutrino, was released. Electric charge conservation requires the neutrino to be electrically neutral, while the angular momentum conservation requires the neutrino to be 1/2 spin like an electron. The first successful decay theory was developed by Enrico Fermi in 1934, based on Pauli's neutrino hypothesis. A modern beta-decay theory, which argues that parity conservation in attenuation interactions is not confirmed, was put forward in 1956 by C. Yang and T. D. Lee, and E. Fermi's beta-decay theory was further developed [33].

With this theory, beta spectrum shapes and half-life times are explained by a rebound and angular correlation experiments. Basis of degradation, metastable states compared to the interactions that generate it can be derived from the transition probability expression. Characteristic times in beta decay (half-lives) are in the order of seconds or longer. Since the natural nuclear time is in the order of 10^{-20}, characteristic times in beta decay are much longer than the natural nuclear time. Degradation by Enrico Fermi, as a result of calculations made by considering it as a weak perturbation, Fermi known as the Golden Rule, which allows the calculation of the rate of transition from one level to another in unit time,

$$\lambda = \frac{2\pi}{\hbar} \left|M_{fi}\right|^2 \rho(E_s) \tag{2.11}$$

it is revealed the relation [26]. In this equation, M_{fi} is the matrix element, λ is the decay rate, $\rho(E_f)$ is the final state density. This matrix element is the integral of the $\widehat{H}_{op}$ interaction between the first and the last quasi-steady states of the system. $\widehat{H}_{op}$ is the Hamilton operator related to the interaction energy that causes the transition;

$$M_{fi} = \int \psi_f^* \widehat{H}_{op} \, \psi_i dv \tag{2.12}$$

Fermi did not use equations (2.11) and (2.12), because he did not know the mathematical expression of matrix element (M) for beta-decay. Instead, he showed that one of the five math processors denoted by Q_X can be used as a substitute for V, using all possible shapes that agree with special relativity. Subindex X gives the shape of the processor Q, i.e. X = V (vector), S (scalar), A (axial vector), P (pseudoscalar) or tensor. It took a lot of time to understand which of the properties of this transformation is suitable for beta decay, and as a result of the experiments, it was concluded that the appropriate result for beta decay was a vector and axial-vector.

The latter state nuclear wave function, φ_V and φ_e represents the time-independent free particle wave functions characterizing the neutrino and the electron. If electron and neutrino wave functions are normalized to V unit volume;

$$\varphi_e(r) = \frac{1}{\sqrt{V}} e^{i\vec{p}_e.\vec{r}/\hbar} = e^{\vec{k}.\vec{r}} \tag{2.13}$$

$$\varphi_v(r) = \frac{1}{\sqrt{V}} e^{i\vec{p}_v.\vec{r}/\hbar} = e^{\vec{k}.\vec{r}} \tag{2.14}$$

It is obtained. If we open these wave functions to series and take the first term to re-translate, this approach would be an allowed approximation. Each subsequent term is called unfavoured allowed according to its degree:

$$e^{i\vec{p}_e.\vec{r}/\hbar} = 1 + \frac{i\vec{p}_e\vec{r}}{\hbar} + \frac{1}{2}\left[\frac{i\vec{p}_e\vec{r}}{\hbar^2}\right]^2 + \cdots \cong= 1 \tag{2.15}$$

$$e^{i\vec{p}_v.\vec{r}/\hbar} = 1 + \frac{i\vec{p}_v\vec{r}}{\hbar} + \frac{1}{2}\left[\frac{i\vec{p}_v\vec{r}}{\hbar^2}\right]^2 + \cdots \cong= 1 \tag{2.16}$$

Some of the theoretical and experimental results of $\beta^{\pm}$ decays of nuclei there are systematic differences. This is the case between the β particle and the product. Coulomb arises from the interaction. Blame in the decay of atoms considering the momentum and positrons and kinetic energy spectra of electrons, this we can conclude. Although in beta-decays of nuclei, electron energy, and momentum

distributions are when the theoretical and experimental results are examined, there are some differences. This is because nuclear the effect of the matrix element is not taken into account in theoretical values.

Theoretical results to obtain a parallel between the experimental data and the effect on the spectrum. The M_{fi} nuclear matrix element, which is assumed to be absent, needs to be taken into account. This is a good approach in terms of compatibility with theoretical results and experimental data.

Sometimes it is in situations where it gives very bad results, in such cases in the approximation, the value of the nuclear matrix element becomes zero. In this case, (2.15) and (2.16) in the plane wave expansion given by equations, other, including momentum dependence, there is impermissible degradation taking into account the terms.

The level of a forbidden decay depends on how many terms we consider after 1 in the plane wave expansion to obtain a non-zero nuclear matrix element. The first term after 1 in the series expansion gives the first-forbidden (FF) decay. The second term is the second-forbidden decay. Generally, a nucleus prefers to decay with an allowed or first-forbidden pass, and it is very difficult to observe higher-order decays.

In this approach, terms that depend on the electron energy and neutrino come from the state densities. Assume we're attempting to calculate the emitted electrons' momentum and energy distribution, the decay rate of the electron, and neutrino [26].

$$d\lambda = \frac{2\pi}{\hbar} g^2 \left|M_{fi}\right|^2 (4\pi)^2 \frac{p_e^2 dp_e q_\nu^2}{\hbar^6} \frac{dq}{dE_f} \tag{2.17}$$

where M_{fi} is the element of the nuclear matrix, E_f is the final state energy, and E_e is a constant.

$$M_{fi} = \int \psi_S^* Q_x \psi_i dv \tag{2.18}$$

$$E_f = E_e + E_v = E_e + q_c \tag{2.19}$$

$$E_e = \frac{dq}{dE_f} = \frac{1}{c} \tag{2.20}$$

In this expression, let's assume the terms that do not contain momentum as constant C. In this case, we can find the distribution of electrons with momentum between p+dp and p from the expression (2.21) [26]:

$$N(p)dp = Cp_e^2 q_v^2 dp \tag{2.21}$$

2.3. THE SELECTION RULES FOR BETA DECAYS

2.3.1. Allowed Decays

In this approach, the wave functions of the neutrino and electron values are used, i.e. it is assumed that the electron and neutrino were created at r = 0 [34]. As long as the electron and neutrino have 0 orbital angular momenta and the nucleus has the same angular momentum, then the angular momentum change is due to the spins of the electron and neutrino. It is spin (s = 1/2) for both neutrino and electron. If these two spins if parallel, total spin (S=1) becomes (S=0) if antiparallel.

If it has an antiparallel spin value according to Fermi (F) decay, there is no difference in nuclear spin value for l = 0 cases ($\Delta I = I_f - I_i = 0$). If the spin values are parallel for neutrino and antineutrino, the total value of angular momentum is 1 according to the Gamow Teller (GT) decay and coupled by forming a vector as ($I_i = I_f + 1$). This is the case if $\Delta I = 0$ or 1 [26]. Parity selection rules and angular momentum for allowed transitions can be summarized as in Table 2.1.

Table 2.1. Selection rules for allowed beta-decay transitions [31].

Transition type	$\Delta J = \lvert J_f - J_i \rvert$	$\pi_i \pi_s$
Fermi	0	+1
Gamow-Teller	1 ($J_i = 0$ or $J_f = 0$)	+1
Gamow-Teller	0, 1 ($J_i > 0$, $J_f > 0$)	+1

Where the first (final) angular momentum and parity operators are represented by J_i (J_f) and π_i (π_f).

2.3.2. Forbidden Decays

Some beta publisher transitions give inaccurate lines for the Curie drawing as opposed to the allowed transitions. The deviation to the incorrect line is because the matrix element is energy-dependent. These transitions are called forbidden transitions. Unlike allowed transitions, forbidden transitions allow the Fermi theory to be tested, as they depend on the matrix element (M) in shape. If the angular moments of the electron and neutrino are different from zero, as the angular momentum increases, the electron and neutrino wave function is strongly suppressed first and with it the decay coefficient decreases. Unlike the nucleus, the monovalent orbital angular momentum of the electron and the neutrino are must be broadcast, so ($\Delta l = \ell + 1 = n + 1$). Where n is the degree of forbidden [35]. The selection rules for forbidden beta transitions can be summarized as follows.

Table 2.2. Selection rules for forbidden beta transitions [36].

Transition type	$\Delta\pi$ (parity change)	Fermi (ΔI)	Gamow-Teller (ΔI)
First forbidden	Yes	0, ±1	0, ±1, ±2
Second forbidden	No	±1, ±2	±2, ±3
Third forbidden	Yes	±2, ±3	±3, ±4
Fourth forbidden	No	±3, ±4	±4, ±5

2.3.3. First Forbidden Decays

Since it is less likely to occur than allowed degradation, forbidden they are called decays. If allowed matrix elements are zero forbidden crossings are possible. Generally, the initial and final states must be of opposite parity for the first-forbidden (FF) decay to occur. Electrons and neutrinos must both be emitting single-value orbital angular momentums relative to a nucleus to satisfy the parity change. The decay of $l = 1$ probability of occurrence is less than $l = 0$ decay, decays with $l = 3, 5, 7$, ... the probability of occurrence is very small. In this case, only $l = 1$ of the forbidden passes considering the degradation, these are called first-forbidden (FF) decays. These decay electron and neutrino with opposite spin (S = 0) Fermi type allowed transitions and parallel spin (S = 1) Gamow-teller (GT) type is similar to forbidden passes. For Gamow-teller (GT) decay of S = 0 to $l = 1$ coupling yields 0, 1, or 2 units of angular momentum, so ($\Delta I = 0, 1,$ or 2). In this case, the selection rules for the first-forbidden (FF) pass are as follows [26]:

$\Delta I = 0, 1, 2$ $\Delta\pi$ (Parity change) =Yes.

The first-forbidden (FF) beta transitions consist of three parts: $\lambda^{\pi} = 0^{-}, 1^{-}, 2^{-}$ exciting transitions. Rank 0 transition contains one relativistic and one non-relativistic matrix element. Rank 1 transition consists of two non-relativistic matrix elements and one relativistic matrix element. The excited state of Rank 2 (rare first-forbidden transitions) consists of a non-relativistic matrix element. Beta-decay transition types are classified according to log*ft* values are given in Table 2.3.

Table 2.3. Classification of beta-decay transition types according to log*ft* values [37].

Transition type	**log*ft***
Super allowed transition	2.9-3.7
Unfavoured allowed transition	3.8-6.0
Allowed transition	≥5.0
Rank 2 unique first-forbidden	8-10

Rank 0, rank 1 first-forbidden	6-9
Second forbidden	11-13
Third forbidden	17-19
Forth forbidden	>22

The *ft* values are given by Equation (2.22) [1],

$$(ft)_{\beta^{\pm}} = \frac{D}{(g_A/g_V)^2 4\pi B\left(I_i \rightarrow I_f, \beta^{\pm}\right)} \tag{2.22}$$

$$D = \frac{2\pi^3 \hbar^2 ln2}{g_v^2 m_e^5 c^4} = 6250\ sec.$$

$$\frac{g_A}{g_V} = -1.254$$

where D and $B\left(I_i \rightarrow I_f, \beta^{\pm}\right)$ are a constant and the transition probability, respectively.

PART 3

FIRST FORBIDDEN $1^- \leftrightarrow 0^+$ BETA TRANSITIONS

The transitions probabilities B($\lambda^{\pi} = 1^-, \beta^{\pm}$) is specified by Bohr and Mottelson [20]:

$$B^{FF}(\lambda^{\pi} = 1^-, \beta^{\pm}) = \left|\langle 1_i^- \left\| M_{\beta^{\pm}}^{FF} \right\| 0^+ \rangle\right|^2 \tag{3.1}$$

where

$$M_{\beta^{\pm}}^{FF} = M^{\pm}(j_v, k = 0, \lambda = 1, \mu) \pm i\frac{m_e c}{\sqrt{3}\hbar}\xi M^{\pm}(\rho_v, \lambda = 1, \mu)$$

$$+i\sqrt{\frac{2}{3}}\frac{m_e c}{\hbar}\xi M^{\pm}(j_A, k = 0, \lambda = 1, \mu) \tag{3.2}$$

3.1. THE CALCULATION OF THE NUCLEAR MATRIX ELEMENTS

In this part of the thesis, detailed mathematical solutions of nuclear beta moment matrix elements of rank 1 excited state are given. Matrix elements of beta moments for 1^- cases of the first-forbidden (FF) transitions (n = 1) are expressed as follows [17].

$$M(\rho_V, \lambda = 1, \mu) = g_V \sum_k t_-(k)\hat{r}_k Y_{1\mu}(\hat{r}_k) \tag{3.3a}$$

$$M(j_V, k = 0, \lambda = 1, \mu) = \frac{1}{\sqrt{4\pi}}\frac{g_V}{c}\sum_k t_-(k)[\,\vec{v}_k\,]_{1\mu} \tag{3.3b}$$

$$M(j_A, k = 0, \lambda = 1, \mu) = g_A \sum_k t_-(k) r_k [Y_1(\hat{r}_k)\vec{\sigma}(k)]_{1\mu} \tag{3.3c}$$

where equations (3.3a) and (3.3b) are the non-relativistic beta moment, equation (3.3c) is the relativistic beta moment.

3.2. THE NON-RELATIVISTIC MATRIX ELEMENT M (ρ_V, λ = 1, μ)

The non-relativistic β moment matrix element in Equation (3.3a) is given as

$$M(\rho_V, \lambda = 1, \mu) = g_V \sum_k t_-(k) \hat{r}_k Y_{1\mu}(\hat{r}_k)$$

In the non-relativistic β moment matrix element equation, g_V is the vector interaction constant, $t_-(k)$ is the isospin reduction operator, r_k is the radius vector of the nucleon, and $Y_{1\mu}(r_k)$ is the spherical harmonic operator. To calculate the matrix element that provides the transformation of the neutron to a proton, the matrix expansion of the operators belonging to the two sub-variables can be applied.

The matrix calculations of the operators of the two sub-variables can be solved with the help of the following expression [38]:

$$\left\langle n_1' j_1' n_2' j_2' j' m' \left| \left\{ \hat{P}_a(1) \otimes \hat{Q}_b(2) \right\}_{c\gamma} \right| n_1 j_1 n_2 j_2 j m \right\rangle = (-1)^{2c} \Pi_{cj} C^{j'm'}_{jmc\gamma}$$

$$\times \begin{Bmatrix} a & b & c \\ j_1' & j_2' & j' \\ j_1 & j_2 & j \end{Bmatrix} \langle n_1' j_1' \| \hat{P}_a(1) \| n_1 j_1 \rangle \langle n_2' j_2' \| \hat{Q}_b(1) \| n_2 j_2 \rangle \, . \tag{3.4}$$

The expression here is the phase, 9j symbol, Clebsch-Gordan coefficient, and reduced matrix elements. In this case, the non-relativistic matrix elements obtain the following expression.

$$\left\langle (l_p s_p) j_p m_p \left| g_V \sum_k t_-(k) \hat{r}_k Y_{1\mu}(\hat{r}_k) \right| (l_n s_n) j_n m_n \right\rangle = (-1)^2 \Pi_{1 j_n} C^{j_p m_p}_{j_n m_n 1\mu}$$

$$\times \begin{Bmatrix} 1 & 0 & 1 \\ l_p & s_p & j_p \\ l_n & s_n & j_n \end{Bmatrix} \langle l_p \| \hat{r}_k Y_{1\mu}(\hat{r}_k) \| l_n \rangle \langle s_p \| \vec{I} \| s_n \rangle \, . \tag{3.5}$$

Let's find each statement in Equation (3.5) separately. The expansion of the expression $\Pi_{abc\ldots}$ is as follows obtained [38]

$$\Pi_{abc..} = \sqrt{(2a+1)(2b+1)(2c+1)\ldots} \tag{3.6}$$

and

$$\Pi_{1j_n} = \sqrt{(2.1+1)(2j_n+1)} = \sqrt{3(2j_n+1)}\ . \tag{3.7}$$

We can use the following expression to reduce the 9j symbol to the 6j symbol obtained [38]

$$\begin{Bmatrix} c & 0 & c \\ d & g & a \\ e & g & b \end{Bmatrix} = \frac{(-1)^{b+d+c+g}}{\sqrt{(2c+1)(2g+1)}} \begin{Bmatrix} a & b & c \\ e & d & g \end{Bmatrix} \tag{3.8}$$

and

$$\begin{Bmatrix} 1 & 0 & 1 \\ l_p & s_p & j_p \\ l_n & s_n & j_n \end{Bmatrix} = \frac{(-1)^{j_n+j_p+1+1/2}}{\sqrt{(2.1+1)(2.\frac{1}{2}+1)}} \begin{Bmatrix} j_n & \frac{1}{2} & 1 \\ l_n & l_p & \frac{1}{2} \end{Bmatrix} = \frac{(-1)^{j_n+j_p-1/2}}{\sqrt{6}} \begin{Bmatrix} j_n & \frac{1}{2} & 1 \\ l_n & l_p & \frac{1}{2} \end{Bmatrix}. \tag{3.9}$$

The expression for the spherical harmonic operator is used [38]

$$\langle l' \| \vec{Y}_L \| l \rangle = \sqrt{\frac{(2L+1)(2l+1)}{4\pi}}\, C^{l'0}_{l0L0}\ . \tag{3.10}$$

In this case, we get this equation

$$\langle l_p \| \vec{Y}_1 \| l_n \rangle = \sqrt{\frac{(2.1+1)(2l_n+1)}{4\pi}}\, C^{l_p0}_{l_n010} = \sqrt{\frac{3(2l_n+1)}{4\pi}} \langle l_n 010 | l_p 0 \rangle\ . \tag{3.11}$$

The following expression is used for the resulting unit operator ($\hat{I}$) [38]

$$\langle s \| \hat{I} \| s' \rangle = \sqrt{2s+1} \tag{3.12}$$

and

$$\langle \tfrac{1}{2} \| \hat{I} \| \tfrac{1}{2} \rangle = \sqrt{2.\tfrac{1}{2}+1} = \sqrt{2}\ . \tag{3.13}$$

When the expressions found for each term are written instead

$$\langle (l_p s_p) j_p m_p | M(\rho_V, \lambda = 1, \mu) | (l_n s_n) j_n m_n \rangle = \sqrt{\frac{3(2j_n+1)(2l_n+1)}{4\pi}}$$

$$\times (-1)^{j_n + j_p - 1/2} \begin{Bmatrix} j_p & j_n & 1 \\ l_p & l_n & \frac{1}{2} \end{Bmatrix} \langle j_n m_n 1\mu | j_p m_p \rangle \langle l_n 010 | l_p 0 \rangle R_{np} \quad . \tag{3.14}$$

The Wigner-Eckart theorem used to the β moment matrix element is a simpler transform into expression. Wigner-Eckart theorem is given as [38]

$$\langle n' j' m' | \hat{M}_{kx} | njm \rangle = (-1)^{2k} C^{j'm'}_{jmkx} \frac{\langle n' j' m' | \hat{M}_{kx} | njm \rangle}{\sqrt{2j'+1}} \tag{3.15}$$

The solution of the β moment matrix element that transforms a neutron into a proton is as follows.

$$\langle (l_p s_p) j_p m_p | M(\rho_V, \lambda = 1, \mu) | (l_n s_n) j_n m_n \rangle = \sqrt{\frac{3(2j_n+1)(2l_n+1)(2j_p+1)}{4\pi}}$$

$$\times \begin{Bmatrix} j_p & j_n & 1 \\ l_p & l_n & \frac{1}{2} \end{Bmatrix} \langle j_n m_n 1\mu | j_p m_p \rangle \langle l_n 010 | l_p 0 \rangle R_{np} \tag{3.16}$$

3.3. THE RELATIVISTIC MATRIX ELEMENT M (j_V, k=0, λ = 1, μ)

The relativistic β moment matrix element in Equation (3.3b) is given as

$$M(j_V, k = 0, \lambda = 1, \mu) = \frac{1}{\sqrt{4\pi}} \frac{g_V}{c} \sum_k t_-(k) [\vec{v}_k]_{1\mu}$$

Here $\vec{v}_k$ is the velocity expression. Firstly, let's get the expression $\vec{v}_k$ velocity.

$$\vec{v} = \dot{\vec{r}} = \frac{i}{\hbar} [\hat{H}, \vec{r}], \tag{3.17}$$

$$\widehat{H} = \frac{\vec{p}^2}{2m} + V_C(\hat{r}) + V_{central}(\hat{r}) + V_{so}(\vec{l}.\vec{s}), \tag{3.18}$$

where $\vec{p}^2/2m$ is the kinetic energy, $V_C(\hat{r})$ is the Coulomb potential; $V_{\text{central}}(\hat{r})$ is the central potential and $V_{so}(\vec{l},\vec{s})$ is the spin-orbit interaction potential. These expressions are as given below

$$V_{central}(\hat{r}) = -V_0 f(r)\left(1 - 2\eta\frac{N-Z}{A}t_z\right),$$

$$f(r) = \frac{1}{1 + e\dfrac{r - R_O}{a}},$$

$$V_C(\hat{r}) = e^2\frac{Z-1}{r}\left\{\frac{2r}{2R_c} - \frac{1}{2}\left(\frac{r}{R_c}\right)^3\right\} \qquad (r \le R_c),$$

$$V_C(\hat{r}) = e^2\frac{Z-1}{r} \qquad (r > R_c),$$

$$V_{so}(\vec{l}.\vec{s}) = -\varepsilon_{ls}\frac{1}{r}\frac{dV_{central(r)}}{dr}$$

$$t_z = 1/2 \ \ (neutrons)\ , \qquad t_z = 1/2 \ \ (protons)$$

After some intermediate operations, we use the following expression for velocity.

$$\vec{v} = -\frac{i\hbar^2}{m}\vec{\nabla} - \frac{i}{\hbar}V_{so}(\vec{r}\times\vec{s}) \tag{3.19}$$

In this case, for the matrix element that changes a neutron into a proton expression is obtained

$$\left\langle (l_p s_p) j_p m_p \left| \frac{1}{\sqrt{4\pi}}\frac{g_V}{c}\sum_k t_-(k)\left[\ \frac{-i\hbar}{m}\vec{\nabla}_{1\mu} + i(\vec{r}\times\vec{s})V_{so}\ \right]_{1\mu} \right| (l_n s_n) j_n m_n \right\rangle \tag{3.20}$$

Equation (3.20) consists of two terms, the operator $\vec{\nabla}$ and $(\vec{r}\times\vec{s})$ cross-product expression. We will calculate these terms separately

$$\langle (l_p s_p) j_p m_p | \vec{\nabla}_{1\mu} | (l_n s_n) j_n m_n \rangle = ? \tag{3.21}$$

$$\langle (l_p s_p) j_p m_p | V_{so} (\vec{r} \times \vec{s})_{1\mu} | (l_n s_n) j_n m_n \rangle = ? \tag{3.22}$$

The following expression is used for the matrix element of the operator $\vec{\nabla}$ [38]:

$$\langle (l_p s_p) j_p m_p | \vec{\nabla}_{1\mu} | (l_n s_n) j_n m_n \rangle = \sqrt{(2j_n + 1)(2j_p + 1)}$$

$$\times \begin{Bmatrix} j_p & j_n & 1 \\ l_n & l_p & \frac{1}{2} \end{Bmatrix} \langle l_p \| \vec{\nabla}_1 \| l_n \rangle \tag{3.23}$$

$$\langle n' l' \| \vec{\nabla}_1 \| n l \rangle = \sqrt{l+1} A_{n' l' n l} \delta_{l' l+1} - \sqrt{l} B_{n' l' n l} \delta_{l' l-1} \tag{3.24}$$

The coefficients A and B in Equation (3.24) are shown as [38]:

$$A_{n' l' n l} = \int_0^\infty \psi^*_{n' l'}(r) \left(\frac{\partial}{\partial r} - \frac{l}{r}\right) \psi_{n l}(r) r^2 dr \tag{3.25}$$

$$B_{n' l' n l} = \int_0^\infty \psi^*_{n' l'}(r) \left(\frac{\partial}{\partial r} + \frac{l+1}{r}\right) \psi_{n l}(r) r^2 dr \tag{3.26}$$

Here $\psi_{nl}(r)$ is the radial part of the corresponding wave function. When the necessary arrangements are made, we can write the $\vec{\nabla}$ operator expression as follows.

$$\eta = \langle l_p \| \vec{\nabla}_1 \| l_n \rangle = \sqrt{(l_n + 1)} A_{l_p l_n} \delta_{l_p l_n + 1} - \sqrt{l_n} B_{l_p l_n} \delta_{l_p l_n + 1} \tag{3.27}$$

Secondly, the following expression is used for the matrix element of vector products [38]:

$$\langle l' s' J' m' \| (\hat{n} \times \hat{s})_k \| l s J m \rangle = i(-1)^{l' + J + s} \delta_{s s'} \sqrt{(2l+1)(2J+1)} C^{l'0}_{l010}$$

$$\times \frac{1}{2} [(J' - l')(J' + l' + 1) - (J - l)(J + l + 1)] \begin{Bmatrix} J' & l' & s \\ l & J & 1 \end{Bmatrix} C^{j'm'}_{jmlk} \tag{3.28}$$

After making the necessary arrangements here, the following equation is obtained:

$$\xi = \langle (l_p s_p) j_p m_p \| V_{so}(\vec{r} \times \vec{s})_{1\mu} \| (l_n s_n j_n) m_n \rangle i(-1)^{l_n + j_n + s_n} \delta_{ss'} \sqrt{(2l_n + 1)(2j_n + 1)}$$

$$\langle l_n 010 | l_p 0 \rangle \frac{1}{2}\left[(j_p - l_p)(j_p + l_p + 1) - (j_n - l_n)(j_n + l_n + 1)\right]$$

$$\times \begin{Bmatrix} j_p & l_p & s_n \\ l_n & j_n & 1 \end{Bmatrix} \langle l_n 010 | l_p 0 \rangle \tag{3.29}$$

When we find $\vec{\nabla}$ and the vector product expressions and substitute (3.20) the equality It can be written as follows.

$$\left\langle (l_p s_p) j_p m_p \left| \frac{1}{\sqrt{4\pi}} \frac{g_V}{c} \sum_k t_-(k) [\ \frac{-i\hbar}{m} \vec{\nabla}_{1\mu} + i(\vec{r} \times \vec{s}) V_{so}\ ]_{1\mu} \right| (l_n s_n) j_n m_n \right\rangle$$

$$= \frac{1}{\sqrt{4\pi}} \frac{g_V}{c} \left[\frac{-i\hbar}{m} \eta + i V_{so} \xi \right]$$

For the solution of the relativistic β moment matrix element, the following equation is obtained [38]:

$$\langle (l_p s_p) j_p m_p | M(j_V, k = 0, \lambda = 1, \mu) | j_n m_p (l_n s_n) \rangle$$

$$= \frac{1}{\sqrt{4\pi}} \frac{g_V}{c} \left\langle (l_p s_p) j_p m_p \left| \frac{-i\hbar^2}{m} \eta + i V_{so} \xi \right| (l_n s_n) j_n m_n \right\rangle R_{np} \tag{3.30}$$

3.4. THE NON-RELATIVISTIC MATRIX ELEMENT M (j_A, k=0, λ = 1, μ)

The non-relativistic β moment matrix element Equation (3.3c) is given as:

$$M(j_A, k = 0, \lambda = 1, \mu) = g_A \sum_k t_-(k) r_k [Y_1(\hat{r}_k) \vec{\sigma}(k)]_{1\mu}$$

where g_A is the axial-vector interaction constant and $\vec{\sigma}(k)$ is the Pauli spin operator. Let's write our statement that changes a neutron into a proton:

$$\langle (l_p s_p) j_p m_p | M(j_A, k=0, \lambda=1, \mu) | (l_n s_n) j_n m_n \rangle$$

$$= \langle (l_p s_p) j_p m_p | g_A \sum_k t_-(k) r_k [Y_1(\hat{r}_k)\vec{\sigma}(k)]_{1\mu} | (l_n s_n) j_n m_n \rangle \quad (3.31)$$

We can calculate the matrix element that changes a neutron into a proton using the matrix expansion of the operators connected to the two sub-variables given in Equation (3.5).

$$\langle (l_p s_p) j_p m_p | g_A \sum_k t_-(k) r_k [Y_1(\hat{r}_k)\vec{\sigma}(k)]_{1\mu} | (l_n s_n) j_n m_n \rangle = (-1)^{2.1} \Pi_{1 j_n} C^{j_p m_p}_{j_n m_n 1\mu}$$

$$\times \begin{Bmatrix} 1 & 0 & 1 \\ l_p & s_p & j_p \\ l_n & s_n & j_n \end{Bmatrix} \langle j_p \| Y_1(\hat{r}_k) \| j_n \rangle \langle s_p \| \vec{\sigma}(k) \| s_n \rangle \quad (3.32)$$

This equality; from phase, symbol 3j, symbol 9j, spherical harmonic, and Pauli spin operator is formed. Let's find each term separately:

$$\Pi_{1 j_n} = \sqrt{3(2j_n + 1)} \quad (3.33)$$

$$\langle l_p \| \vec{Y}_1 \| l_n \rangle = \sqrt{\frac{3(2l_n+1)}{4\pi}} \langle l_n 010 | l_p 0 \rangle \quad (3.34)$$

The following transformation is used for the resulting Pauli spin matrix element operator [38]:

$$\langle s' \| \hat{S}_1 \| s \rangle = \delta_{ss'} \sqrt{s(s+1)(2s+1)} \quad (3.35)$$

and

$$\langle s_p \| \hat{S}_1 \| s_n \rangle = \delta_{ss'} \sqrt{\tfrac{1}{2}(\tfrac{1}{2}+1)(2.\tfrac{1}{2}+1)} = \sqrt{\tfrac{3}{2}} \quad (3.36)$$

Since $\vec{\sigma} = 2\hat{S}$, it is found as $\vec{\sigma} = \sqrt{6}$. After writing each term in its place, Equation (3.37) is obtained for the non-relativistic β moment matrix element.

$$= \sqrt{\frac{54}{4\pi}(2l_n+1)(2j_n+1)} \begin{Bmatrix} 1 & 0 & 1 \\ l_p & s_p & j_p \\ l_n & s_n & j_n \end{Bmatrix} \langle l_n 010 | l_p 0 \rangle \tag{3.37}$$

By using the Wigner-Eckart theorem, we obtain the reduced nuclear matrix element as follows.

$$\langle (l_p s_p) j_p m_p | M(j_A, k=0, \lambda=1, \mu) | (l_n s_n) j_n m_n \rangle$$

$$= \sqrt{\frac{54}{4\pi}(2l_n+1)(2j_n+1)(2j_p+1)} \begin{Bmatrix} 1 & 0 & 1 \\ l_p & s_p & j_p \\ l_n & s_n & j_n \end{Bmatrix} \langle l_n 010 | l_p 0 \rangle R_{np} \tag{3.38}$$

Where R_{np} expression is as follows.

$$R_{np} = \int_0^\infty U_p^*(r) U_n(r) r^3 \, dr \tag{3.39}$$

Here R_{np} is the radial part of the wave function [38].

PART 4

THE pn QUASI-PARTICLE RANDOM PHASE APPROXIMATION

4.1. THE pn-QRPA FOR RANK 1 TRANSITIONS

Halbleib and Sorensen developed the quasi-particle random phase approximation (QRPA), which describes excitations created by a charge-exchanging transition operator, by generalizing the usual RPA [11]. In this part of the thesis, the solutions for the proton-neutron quasi-particle random phase approximation(pn-QRPA) we use to obtain the eigenvalues and eigenfunctions of the total Hamilton operator for rank 1 ($\lambda^{\pi} = 1^{-}$), first-forbidden (FF) beta transitions are given in detail. The model Hamilton operator is generally as follows:

$$\widehat{H} = \widehat{H}_{sqp} + \hat{h}_{ph} \tag{4.1}$$

The system's single quasi-particle Hamiltonian ($\widehat{H}_{sqp}$) is shown by

$$\widehat{H}_{sqp} = \sum_{j,m,\tau} \varepsilon_j(\tau)\hat{\alpha}^{+}_{jm}(\tau)\hat{\alpha}_{jm}(\tau), \qquad \tau = n, p \tag{4.2}$$

Where $\varepsilon_j(\tau)$ and $\hat{\alpha}^{+}_{jm}(\tau)$ ($\hat{\alpha}_{jm}(\tau)$) are the single quasi-particle energy of the nucleons with angular momentum (j_τ) and the quasi-particle creation (annihilation) operators, respectively. The $\hat{h}_{ph}$ is the spin-isospin effective interaction Hamiltonian which generates 1^{-} vibration modes in the particle-hole channel and is shown as

$$\begin{aligned}\hat{h}_{ph} = \frac{2\chi_{ph}}{g_A^2} \sum_{j_p j_n j_{p'} j_{n'} \mu} & \left\{ b_{j_p j_n} A^{+}_{j_p j_n}(\lambda\mu) + (-1)^{\lambda-\mu} \bar{b}_{j_p j_n} A_{j_p j_n}\,(\lambda-\mu) \right\} \\ & \times \left\{ b_{j_{p'} j_{n'}} A_{j_{p'} j_{n'}}(\lambda\mu) + (-1)^{\lambda-\mu} \bar{b}_{j_{p'} j_{n'}} A^{+}_{j_{p'} j_{n'}}(\lambda-\mu) \right\} \\ = 2\chi_{ph} \sum_{\mu} & T^{+}_{\lambda\mu}\, T^{-}_{\lambda\mu}\end{aligned} \tag{4.3}$$

Where $T^{-}_{\lambda\mu}(T^{+}_{\lambda\mu})$ rank 1 is the first-forbidden (FF) beta transition annihilation operator, and χ_{ph} is particle-hole effective interaction constant [1,20].

$$T^{-}_{\lambda\mu} = \sum_{j_p j_n m_p m_n} \langle j_p m_p (l_p s_p) | r^{\lambda} y_{\lambda\mu} | j_n m_n (l_n s_n) \rangle \, a^{+}_{j_p m_p} a_{j_n m_n} \tag{4.4}$$

In the second quantization space, it is given as in Equation (4.4). When the rank 1 transition operator is rewritten according to the resulting Wigner-Eckart theorem:

$$T^{-}_{\lambda\mu} = \sum_{j_p j_n} \frac{\langle j_p (l_p s_p) \| r^{\lambda} y_{\lambda} \| j_n (l_n s_n) \rangle}{\sqrt{2j_p+1}} \sum_{m_p m_n} \langle j_n m_n \lambda\mu | j_p m_p \rangle \, a^{+}_{j_p m_p} a_{j_n m_n} \tag{4.5}$$

Where $a^{+}_{j_p m_p}$ and $a_{j_n m_n}$ are particle generation and elimination operators.

$$a^{+}_{j_p m_p} = U_{jp} \alpha^{+}_{j_p m_p} + (-1)^{j_p - m_p} V_{jp} \alpha_{j_P - m_P} \tag{4.6}$$

$$a_{j_n m_n} = U_{jn} \alpha_{j_n m_n} + (-1)^{j_n - m_n} V_{jn} \alpha^{+}_{j_n - m_n} \tag{4.7}$$

$\alpha^{+}_{j_p m_p}$, and $\alpha_{j_n m_n}$ are the particle generation and elimination operators, U_{jp} and V_{jp} are the probability amplitudes of the hole and particle states in a given j state [37]. $a^{+}_{j_p m_p}$, and $a_{j_n m_n}$ particle production, a product of annihilation operators

$$\begin{aligned} a^{+}_{j_p m_p} a_{j_n m_n} = {} & (-1)^{j_n - m_n} U_{jp} V_{jn} \alpha^{+}_{j_p m_p} \alpha^{+}_{j_n - m_n} \\ & + (-1)^{j_p - m_p} U_{jn} V_{jp} \alpha_{j_P - m_P} \alpha_{j_n m_n} \end{aligned} \tag{4.8}$$

It is obtained in the form. In this case, the beta transition operator is as follows:

$$\begin{aligned} & T^{-}_{\lambda\mu} = \\ & \sum_{j_p j_n} \frac{\langle j_p (l_p s_p) \| r^{\lambda} y_{\lambda} \| j_n (l_n s_n) \rangle}{\sqrt{2j_p+1}} \Big\{ U_{jp} V_{jn} \sum_{m_p m_n} (-1)^{j_n - m_n} \langle j_n m_n \lambda\mu | j_p m_p \rangle \alpha^{+}_{j_p m_p} \alpha^{+}_{j_n - m_n} + \\ & U_{jn} V_{jp} \sum_{m_p m_n} (-1)^{j_p - m_p} \langle j_n m_n \lambda\mu | j_p m_p \rangle \alpha_{j_P - m_P} \alpha_{j_n m_n} \Big\} \end{aligned} \tag{4.9}$$

Where $A^{+}_{j_p j_n}(\lambda\mu)$ and $A_{j_p j_n}$ $(\lambda\mu)$ are boson generation and annihilation operators.

$$A^{+}_{j_p j_n}(\lambda\mu) = \sqrt{\frac{2\lambda+1}{2j_p+1}}\sum_{m_p m_n}(-1)^{j_n-m_n}\langle j_n m_n \lambda\mu | j_p m_p\rangle \alpha^{+}_{j_p m_p}\alpha^{+}_{j_n-m_n} \quad (4.10)$$

$$\left[A^{+}_{j_p j_n}(\lambda\mu)\right]^{+} = A_{j_p j_n}(\lambda\mu) \quad (4.11)$$

$$A_{j_p j_n}(\lambda\mu) = \sqrt{\frac{2\lambda+1}{2j_p+1}}\sum_{m_p m_n}(-1)^{j_n-m_n}\langle j_n m_n \lambda\mu | j_p m_p\rangle \alpha_{j_n-m_n}\alpha_{j_p m_p} \quad (4.12)$$

The rank 1 beta transition operator in terms of boson removal and generation operators is obtained as follows;

$$T^{-}_{\lambda\mu} = \sum_{j_p j_n}\frac{\langle j_p(l_p s_p)\|r^{\lambda}y_{\lambda}\|j_n(l_n s_n)\rangle}{\sqrt{2\lambda+1}} \times\left\{V_{jn}U_{jp}A^{+}_{j_p j_n}(\lambda\mu) + V_{jp}U_{jn}(-1)^{\lambda-\mu}A_{j_p j_n}(\lambda-\mu)\right\} \quad (4.13)$$

$$b_{j_p j_n} = \frac{\langle j_p(l_p s_p)\|r^{\lambda}y_{\lambda}\|j_n(l_n s_n)\rangle}{\sqrt{2\lambda+1}}V_{jn}U_{jp} \quad (4.14a)$$

$$\bar{b}_{j_p j_n} = \frac{\langle j_p(l_p s_p)\|r^{\lambda}y_{\lambda}\|j_n(l_n s_n)\rangle}{\sqrt{2\lambda+1}}U_{jn}V_{jp} \quad (4.14b)$$

With the reduced beta moment matrix elements $b_{j_p j_n}$ and $\bar{b}_{j_p j_n}$the beta transition elimination operator is obtained as follows:

$$T^{-}_{\lambda\mu} = \sum_{j_p j_n}\left\{b_{j_p j_n}A^{+}_{j_p j_n}(\lambda\mu) + (-1)^{\lambda-\mu}\bar{b}_{j_p j_n}A_{j_p j_n}(\lambda-\mu)\right\} \quad (4.15a)$$

Since $(T^{-}_{\lambda\mu})^{+} = T^{+}_{\lambda\mu}$ beta transition generation operator

$$T^{+}_{\lambda\mu} = \sum_{j_p j_n}\left\{b_{j_p j_n}A_{j_p j_n}(\lambda\mu) + (-1)^{\lambda-\mu}\bar{b}_{j_p j_n}A^{+}_{j_p j_n}(\lambda-\mu)\right\} \quad (4.15b)$$

It is obtained as [37]. One particle Hamilton operator is given as

$$H_{S\theta P} = \sum_{j,\sigma}\varepsilon_j(\sigma)B_j(\sigma)\ ; \qquad (\sigma = p,n) \quad (4.16)$$

$B_j(\sigma) = \sum_m \alpha_{jm}^{+}(\sigma)\alpha_{jm}(\sigma)$

generally defined as above. When written in detail for each nucleon

$$H_{S\theta P} = \sum_{jp'} \varepsilon_{jp'} B_{jp'} + \sum_{jp'} \varepsilon_{jn'} B_{jn'} \tag{4.17}$$

$$B_{jp'} = \sum_{mp'} \alpha^{+}_{jp'mp'} \alpha_{jp'mp'} \tag{4.18a}$$

$$B_{jn'} = \sum_{mp'} \alpha^{+}_{jn'mn'} \alpha_{jn'mn'} \tag{4.18b}$$

equations are obtained.

The total Hamilton operator of the system consists of the sum of the single-particle Hamilton operator and the effective interaction Hamilton of rank 1 excited state.

$$H = H_{S\theta P} + H_{\text{effective}} \tag{4.19}$$

Since rank 1 excited state consists of a matrix element, there is separate active interaction Hamilton operators. This is given as

$$H_{\text{effective}} = h_1 \tag{4.20}$$

$$h_1 = 2X_{11} \sum_{j_{p_1} j_{n_1} j_{p_2} j_{n_2} \mu} \begin{Bmatrix} \left[b_{j_{p_1} j_{n_1}} A^{+}_{j_{p_1} j_{n_1}} (\lambda\mu) + (-1)^{\lambda-\mu} \bar{b}_{j_{p_1} j_{n_1}} A_{j_{p_1} j_{n_1}} (\lambda - \mu) \right] \\ \left[b_{j_{p_2} j_{n_2}} A_{j_{p_2} j_{n_2}} (\lambda\mu) + (-1)^{\lambda-\mu} \bar{b}_{j_{p_2} j_{n_2}} A^{+}_{j_{p_2} j_{n_2}} (\lambda - \mu) \right] \end{Bmatrix} \tag{4.21}$$

The equation-of-motion (EOM) of the system in general

$$[H, Q_i^{+}] = \omega_i Q_i^{+} \tag{4.22}$$

It is obtained in the form. Here ω_i is the ground state energy of the neighbouring nucleus. Q_i^+ is the phonon generation operator in the quasi-particle space and is written in terms of boson operators as follows [37];

$$Q_i^+(\lambda\mu) = \sum_{j_p j_n}\left[\mathrm{r}^i_{j_p j_n} A^+_{j_p j_n}(\lambda\mu) - (-1)^{\lambda-\mu}\delta^i_{j_p j_n} A_{j_p j_n}(\lambda\mu)\right] \quad (4.23a)$$

$$\left[Q_i(\lambda\mu), Q^+_{i'}(\lambda'\mu')\right] = \delta_{ii'}\delta_{\lambda\lambda'}\delta_{\mu\mu'} \quad (4.23b)$$

The normalization condition in terms of $\mathrm{r}^i_{j_p j_n}$ and $S^i_{j_p j_n}$ wave functions are given as follows.

$$\sum_{j_p j_n}\left\{\left(\mathrm{r}^i_{j_p j_n}\right)^2 - \left(S^i_{j_p j_n}\right)^2\right\} = 1 \quad (4.24)$$

4.2. THE pn-QRPA EQUATION

The proton-neutron quasi-particle random phase approximation (pn-QRPA) equation by using the equations-of-motion (EOM) method can be derived. The basic excitation is defined as

$$|\omega\rangle = Q^+_\omega |pnQRPA\rangle \quad (4.25)$$

Where the phonon creation operator in the proton-neutron quasi-particle random phase approximation (pn-QRPA) is given as

$$Q^+_\omega = \sum_{pn}\left[X^\omega_{pn} A^+_{pn}(JM) - Y^\omega_{pn}\tilde{A}_{pn}(JM)\right] \quad (4.26)$$

and $|pnQRPA\rangle$ is the proton-neutron quasi-particle random phase approximation (pn-QRPA) vacuum. Where $\omega = kJ^\pi$ contains k and J^π are the eigenvalue index and the spin–parity, respectively. The matrix elements of A and B are shown as

$$A_{pn,p'n'}(J) = \left(E_p + E_n\right)\delta_{pp'}\delta_{nn'} + \left(u_p u_n u_{p'} u_{n'} + v_p v_n v_{p'} v_{n'}\right)\langle pn; J|V|p'n'; J\rangle$$

$$+\left(u_p v_n u_{p'} v_{n'} + v_p u_n v_{p'} u_{n'}\right)\left\langle pn^{-1}; J\middle|V_{RES}\middle|p'n'^{-1}; J\right\rangle \quad (4.27)$$

$$B_{pn,p'n'}(J) = -\left(u_p u_n v_{p'} v_{n'} + v_p v_n u_{p'} u_{n'}\right)\langle pn; J|V|p'n'; J\rangle$$

$$+\left(u_p v_n v_{p'} u_{n'} + v_p u_n u_{p'} v_{n'}\right)\left\langle pn^{-1}; J\middle|V_{RES}\middle|p'n'^{-1}; J\right\rangle \quad (4.28)$$

The particle-hole elements of the matrix $\langle pn^{-1}; J|V_{RES}|p'n'^{-1}; J\rangle$

$$\left\langle pn^{-1}; J\middle|V_{RES}\middle|p'n'^{-1}; J\right\rangle = -\sum_{J'} \hat{J'}^2 \begin{Bmatrix} j_p & j_n & J \\ j_{p'} & j_{n'} & J' \end{Bmatrix} \langle pn'; J|V|p'n; J\rangle \quad (4.29)$$

The proton-neutron quasi-particle random phase approximation (pn-QRPA) equations are given as

$$\sum_{p'n'} A_{pn,p'n'} X^{\omega}_{p'n'} + \sum_{p'n'} B_{pn,p'n'} Y^{\omega}_{p'n'} = E_{\omega} X^{\omega}_{pn} \quad (4.30)$$

$$-\sum_{p'n'} (B^{+})_{pn,p'n'} X^{\omega}_{p'n'} + \sum_{p'n'} (A^{T})_{pn,p'n'} Y^{\omega}_{p'n'} = E_{\omega} Y^{\omega}_{pn} \quad (4.31)$$

The equation of quasi-particle random phase approximation (QRPA) and random phase approximation (RPA) matrix are given by

$$\begin{pmatrix} A & B \\ -B^{*} & -A^{*} \end{pmatrix} \begin{pmatrix} X^{\omega} \\ Y^{\omega} \end{pmatrix} = E_{\omega} \begin{pmatrix} X^{\omega} \\ Y^{\omega} \end{pmatrix} \quad (4.32)$$

This equation is a non-Hermitian eigenvalue problem. As in the case of the quasi-particle random phase approximation (QRPA), B is symmetric and A is Hermitian. The proton-neutron quasi-particle random phase approximation (pn-QRPA) matrix receives the same form as this equation (4.32) [39].

4.3. THE pn-QRPA FORMULA SOLUTIONS PROPERTY

The annihilation condition can be used to determine the composition of the proton-neutron quasi-particle random phase approximation (pn-QRPA) vacuum.

$$Q_\omega|pnQRPA\rangle = 0 \qquad \text{for all } \omega, \tag{4.33}$$

where

$$Q_\omega = \sum_{pn}\left[X_{pn}^{\omega^*}A_{pn}(JM) - Y_{pn}^{\omega^*}\tilde{A}_{pn}^{+}(JM)\right]. \tag{4.34}$$

The proton-neutron quasi-particle random phase approximation (pn-QRPA) orthonormality condition is shown as

$$\sum_{pn}\left(X_{pn}^{kJ^{\pi}*}X_{pn}^{k'J^{\pi}} - Y_{pn}^{kJ^{\pi}*}Y_{pn}^{k'J^{\pi}}\right) = \delta_{kk'} \qquad (pn-QRPA \text{ orthonormality}) \tag{4.35}$$

The proton-neutron quasi-particle random phase approximation (pn-QRPA) normalization condition is shown as

$$\sum_{pn}\left(\left|X_{pn}^{\omega}\right|^2 - \left|Y_{pn}^{\omega}\right|^2\right) = 1 \tag{4.36}$$

The completeness relations for the proton-neutron quasi-particle random phase approximation (pn-QRPA) is [39], as shown as

$$\sum_{pn}\left(X_{pn}^{kJ^{\pi}}X_{p'n'}^{kJ^{\pi}*} - Y_{pn}^{kJ^{\pi}*}Y_{p'n'}^{kJ^{\pi}}\right) = \delta_{pp'}\delta_{nn'}\,, \tag{4.37}$$

Which is the proton-neutron quasi-particle random phase approximation (pn-QRPA)'s completeness relation I. The completeness relation II of the proton-neutron quasi-particle random phase approximation (pn-QRPA) is given as

$$\sum_{k}\left(X_{pn}^{kJ^{\pi}}Y_{p'n'}^{kJ^{\pi_*}}-Y_{pn}^{kJ^{\pi_*}}X_{p'n'}^{kJ^{\pi}}\right)=0 \tag{4.38}$$

The matrix equation is developed by combining equations (4.37) and (4.38) are given as

$$\sum_{\substack{n\\E_n>0}}\left[\binom{X^{\omega}}{Y^{\omega}}(X^{\omega+},-Y^{\omega+})-\binom{Y^{\omega*}}{X^{\omega*}}(Y^{\omega T},-X^{\omega T})\right]=\begin{pmatrix}1 & 0\\ 0 & 1\end{pmatrix} \tag{4.39}$$

The proton-neutron quasi-particle random phase approximation (pn-QRPA) equation, like the random phase approximation (RPA) and quasi-particle random phase approximation (QRPA) equations, also has positive and negative energy solutions [39]. The condition form is

$$\left|Y_{pn}^{\omega}\right|\ll 1 \qquad \text{for all } \omega, \text{pn.} \tag{4.40}$$

The proton-neutron quasi-particle random phase approximation (pn-QRPA) solutions are similar to the corresponding proton-neutron quasi-particle Tamm–Dancoff approximation (pn-QTDA) solutions under this condition. That is shown by

$$|pnQRPA\rangle=|BCS\rangle+\text{small corrections} \tag{4.41}$$

The corrections are two-neutron-quasiparticle-two-proton-quasiparticle, four-neutron-quasiparticle-four-proton-quasiparticle, etc., components.

The proton-neutron quasi-particle random phase approximation (pn-QRPA) in the ground state

$$|pnQRPA\rangle=\mathcal{N}_0 e^{S}|BCS\rangle \tag{4.42}$$

where N_0 is a factor of normalization and

$$S = \frac{1}{2}\sum_{JM}\sum_{\substack{pn \\ p'n'}} C_{pnp'n'}(J)\, A^{+}_{pn}(JM)\tilde{A}^{+}_{p'n'}(JM)\,, \qquad C_{p'n'pn}(J) = C_{pnp'n'}(J) \quad (4.43)$$

In the following equation, the amplitudes X and Y are solved, as shown as

$$\sum_{pn} X^{\omega *}_{pn}\, C_{pnp'n'}(J) = Y^{\omega *}_{p'n'} \qquad \text{for all } p'n', \omega \quad (4.44)$$

The C coefficients are obtained by solving this series of linear equations [39]. We can see from (4.42) and (4.43) that the Bardeen–Cooper–Schrieffer theory (BCS) vacuum is the first term of the proton-neutron quasi-particle random phase approximation (pn-QRPA) vacuum, and the rest are k-neutron-quasiparticle- k-proton-quasiparticle terms for k = 2, 4, 6,...

The one-quasiparticle densities (4.45) and (4.46) provide a way to build on the proton-neutron quasi-particle random phase approximation (pn-QRPA) classification to achieve higher-pnQRPA frameworks, as shown as

$$\langle pnQRPA|a^{+}_{\pi}a_{\pi}|pnQRPA\rangle = \hat{j}_{p}^{-2}\sum_{\substack{kJ \\ E_k>0}}\hat{J}^{2}\sum_{n}\left|Y^{kJ^{\pi}}_{pn}\right|^{2} \quad (4.45)$$

$$\langle pnQRPA|a^{+}_{\nu}a_{\nu}|pnQRPA\rangle = \hat{j}_{n}^{-2}\sum_{\substack{kJ \\ E_k>0}}\hat{J}^{2}\sum_{p}\left|Y^{kJ^{\pi}}_{pn}\right|^{2} \quad (4.46)$$

In this case, the equations-of-motion (EOM) may be used with the accurate ground state to obtain the exact A and B matrices, as shown as

$$A_{pn,p'n'} \equiv \left\langle pnQRPA\middle|\left[A_{pn}, \mathcal{H}, A^{+}_{p'n'}\right]\middle|pnQRPA\right\rangle, \quad (4.47)$$

$$B_{pn,p'n'} \equiv \langle pnQRPA|\left[A_{pn}, \mathcal{H}, \tilde{A}_{p'n'}\right]|pnQRPA\rangle\,. \quad (4.48)$$

The higher-pnQRPA equations are then solved in a self-consistent, iterative manner. In any approximation, the matrix elements Equations (4.47) and (4.48) are evaluated. The approximation used for one-quasiparticle densities determines the level of approximation. The self-consistent problem is written in the lowest order as follows [39]:

$$\begin{pmatrix} \bar{A} & \bar{B} \\ -\bar{B}^{*} & -\bar{A}^{*} \end{pmatrix} \begin{pmatrix} \bar{X}^{\omega} \\ \bar{Y}^{\omega} \end{pmatrix} = E_{\omega} \begin{pmatrix} \bar{X}^{\omega} \\ \bar{Y}^{\omega} \end{pmatrix} \tag{4.49}$$

The barred matrices B, A, Y, and X are the normal matrices B, A, Y, and X multiplied by combinations of densities of the one-quasiparticle Equations (4.45) and (4.46) as defined in [40], which also introduces a renormalized proton-neutron quasi-particle random phase approximation (pn-QRPA or pn-RQRPA) theory [39].

4.4. THE β-DECAY TRANSITIONS IN THE pn-QRPA FRAMEWORK

This section discusses the β-decay transitions between states of the neighbouring even-even reference nucleus and an open-shell odd-odd nucleus. Consider transitions from an odd-odd nucleus's initial state Equation (4.25) to the even-even reference nucleus's ground state $|pnQRPA\rangle$. For β^{-} and β^{+} transitions, the decay amplitude is given

$$\begin{aligned} \langle pnQRPA|\beta^{\mp}_{LM}|\omega\rangle &= \langle pnQRPA|\beta^{\mp}_{LM}Q^{+}_{\omega}|pnQRPA\rangle \\ &= \langle pnQRPA|\left[\beta^{\mp}_{LM}, Q^{+}_{\omega}\right]|pnQRPA\rangle . \end{aligned} \tag{4.50}$$

We have used the commutator to access the Y terms of the proton-neutron quasi-particle random phase approximation (pn-QRPA) phonon, as is customary in the random phase approximation (RPA) work [39]. The β^{-} operator's quasi-particle representation as

$$\begin{aligned} \beta^{-}_{LM} = \sum_{pn} \mathcal{M}_{L}(pn)\{ & u_p v_n A^{+}_{pn}(LM) + v_p u_n \tilde{A}_{pn}(LM) \\ & + u_p u_n \left[a^{+}_{p}\tilde{a}_{n}\right]_{LM} + (-1)^{j_p+j_n+L} v_p v_n \left[a^{+}_{n}\tilde{a}_{p}\right]_{LM}\} . \end{aligned} \tag{4.51}$$

$$\beta_{LM}^{-} = \hat{L}^{-1} \sum_{pn} (p\|B_L\|n)\left[c_p^{+}\tilde{c}_n\right]_{LM} = \sum_{pn} \mathcal{M}_L\,(pn)\left[c_p^{+}\tilde{c}_n\right]_{LM}. \tag{4.52}$$

By taking the Hermitian conjugate of this and applying by the Wigner-Eckart theorem,

$$(\beta_{LM}^{-})^{+} = (-1)^{M}\beta_{L,-M}^{+}, \tag{4.53}$$

where

$$\beta_{LM}^{+} = \hat{L}^{-1} \sum_{np} (n\|B_L\|p)\left[c_n^{+}\tilde{c}_p\right]_{LM} = \sum_{np} \mathcal{M}_L\,(np)\left[c_n^{+}\tilde{c}_p\right]_{LM}. \tag{4.54}$$

Combining equation (4.53) with the converse relation we have

$$\left(\beta_{LM}^{\mp}\right)^{+} = (-1)^{M}\beta_{L,-M}^{\mp}. \tag{4.55}$$

The Condon-Shortley Phase Layout (CS) and Biedenharn-Rose Phase Layout (BR) phase conventions have the same allowed β-decay relations. Due to spatial dependence, the forbidden unique decay has a convention-dependent phase factor [39]. The quasi-boson approximation (QBA) given as

$$\begin{aligned}
&\langle pnQRPA|\beta_{LM}^{-}|\omega\rangle \underset{\approx}{QBA} \langle BCS|[\beta_{LM}^{-}, Q_{\omega}^{+}]|BCS\rangle \\
&= \sum_{\substack{pn \\ p'n'}} \mathcal{M}_L\,(p'n')\Big\{v_{p'}u_{n'}\,X_{pn}^{\omega}\left\langle BCS\middle|\left[\tilde{A}_{p'n'}(LM), A_{pn}^{+}(JM_{\omega})\right]\middle|BCS\right\rangle \\
&\qquad\qquad -u_{p'}v_{n'}Y_{pn}^{\omega}\left\langle BCS\middle|\left[A_{p'n'}^{+}(LM), \tilde{A}_{pn}(JM_{\omega})\right]\middle|BCS\right\rangle\Big\},
\end{aligned} \tag{4.56}$$

We use the notation Mω, To distinguish the z projection of J from the z projection of L. The matrix elements show Kronecker deltas so that

$$\begin{aligned}
&\langle pnQRPA|\beta_{LM}^{-}|\omega\rangle \\
&\qquad = \delta_{LJ}\delta_{M,-M_{\omega}}(-1)^{L+M}\sum_{pn} \mathcal{M}_L\,(pn)\left(v_p u_n X_{pn}^{\omega} + u_p v_n Y_{pn}^{\omega}\right).
\end{aligned} \tag{4.57}$$

The transition amplitude is determined by the Wigner–Eckart theorem,

$$(pnQRPA\|\beta_L^-\|\omega) = \delta_{LJ}\hat{L}\sum_{pn}\mathcal{M}_L\,(pn)\big(\upsilon_p u_n X_{pn}^{\omega} + u_p \upsilon_n Y_{pn}^{\omega}\big). \tag{4.58}$$

We use equation (4.55) to discover the transition amplitude for β^+ decay, which gives:

$$\begin{aligned}\langle pnQRPA|\beta_{LM}^+|\omega\rangle \;&=\; (-1)^M \left\langle pnQRPA\middle|\left(\beta_{L,-M}^-\right)^+\middle|\omega\right\rangle \\ &=\; (-1)^M \left\langle\omega\middle|\beta_{L,-M}^-\middle|pnQRPA\right\rangle^* = (-1)^M\left\langle\omega\middle|\beta_{L,-M}^-\middle|pnQRPA\right\rangle, \end{aligned}\tag{4.59}$$

Where we have assumed that matrix elements are real as is usual. In the same way as equation (4.56), this becomes

$$\begin{aligned}\langle pnQRPA|\beta_{LM}^+|\omega\rangle \;&\overset{QBA}{\approx}\; (-1)^M \left\langle BCS\middle|\left[Q_\omega^+, \beta_{L,-M}^-\right]\middle|BCS\right\rangle \\ &= \sum_{\substack{pn\\ p'n'}} \mathcal{M}_L\,(p'n')\Big\{\upsilon_{p'}u_{n'}\,X_{pn}^{\omega}\left\langle BCS\middle|\left[A_{pn}(JM_\omega), A_{p'n'}^+(L,-M)\right]\middle|BCS\right\rangle \\ &\qquad -u_{p'}\upsilon_{n'}Y_{pn}^{\omega}\left\langle BCS\middle|\left[\hat{A}_{pn}^+(JM_\omega), \tilde{A}_{p'n'}(L,-M)\right]\middle|BCS\right\rangle\Big\} \\ &= \delta_{LJ}\delta_{M,-M_\omega}(-1)^M \textstyle\sum_{pn}\mathcal{M}_L\,(pn)\big(u_p\upsilon_n X_{pn}^{\omega} + \upsilon_p u_n Y_{pn}^{\omega}\big). \end{aligned}\tag{4.60}$$

By using the Wigner–Eckart theorem to obtain the reduced matrix element, as shown as

$$(pnQRPA\|\beta_L^+\|\omega) = \delta_{LJ}(-1)^L\hat{L}\sum_{pn}\mathcal{M}_L\,(pn)\big(u_p\upsilon_n X_{pn}^{\omega} + \upsilon_p u_n Y_{pn}^{\omega}\big). \tag{4.61}$$

We use the relation for transitions in the opposite direction equation (4.55). For β^- transitions it gives as

$$\langle\omega|\beta^{-}_{LM}|pnQRPA\rangle = (-1)^{M}\left\langle\omega\left|\left(\beta^{+}_{L,-M}\right)^{+}\right|pnQRPA\right\rangle = (-1)^{M}\langle pnQRPA\left|\beta^{+}_{L,-M}\right|\omega\rangle$$
$$= \delta_{LJ}\delta_{M\,M_{\omega}}\sum_{pn}\mathcal{M}_{L}\,(pn)\left(u_{p}v_{n}X^{\omega}_{pn} + v_{p}u_{n}Y^{\omega}_{pn}\right), \qquad (4.62)$$

where the last step came from equation (4.62) [39]. As a result, the reduced matrix element is shown as

$$\left(\omega\left\|\beta^{-}_{L}\right\|pnQRPA\right) = \delta_{LJ}\,\hat{L}\sum_{pn}\mathcal{M}_{L}\,(pn)\left(u_{p}v_{n}X^{\omega}_{pn} + v_{p}u_{n}Y^{\omega}_{pn}\right). \qquad (4.63)$$

The remaining transition amplitude is calculated similarly using equation (4.57) [39], with the result

$$\left(\omega\left\|\beta^{+}_{L}\right\|pnQRPA\right) = \delta_{LJ}(-1)^{L}\hat{L}\sum_{pn}\mathcal{M}_{L}\,(pn)\left(v_{p}u_{n}X^{\omega}_{pn} + u_{p}v_{n}Y^{\omega}_{pn}\right). \qquad (4.64)$$

PART 5

RESULTS AND DISCUSSION

For some spherical nuclei in the $186 \leqslant A \leqslant 202$ mass region for Gold (Au), from $0^{+} \leftrightarrow 1^{-}$ first-forbidden (FF) β moment matrix elements investigated. Beta transition strength distributions are very important in the accurate determination of log*ft* values, which greatly contribute to the understanding of nuclear beta decay. The relativistic matrix element of the first-forbidden (FF) beta-transition operators are calculated directly without any assumptions.

The contribution of the forbidden transitions, which have longer half-lives and less probability of occurrence than the allowed decays, to the ground state transitions is very effective in determining the total beta transition half-life times.

The *ft* function is inversely proportional to the square of the nuclear transition matrix element $|M|^2$. The larger *ft*, i.e. the smaller square of the nuclear transition matrix element $|M|^2$, the more impossible the transition under consideration, i.e. it is forbidden. If the square of the nuclear transition matrix element $|M|^2$ is proportional to the degree of overlap of the wavefunctions of the mother nucleus and the product nucleus. The more the wavefunctions overlap, the larger square of the nuclear transition matrix element $|M|^2$ becomes and approaches 1. The size of the nuclear matrix element (M) depends on the selection rules and the magnitude of the orbital angular momentum (l). Log*ft* values of beta transitions, which are important in understanding the nuclear structure of first-forbidden (FF) transitions with $\lambda^{\pi} = 1^{-}$ have a significant contribution to the determination of half-life times, the explanation of double beta decay processes with two neutrinos and nuclear astrophysical events. Because the investigation of charge-change collective excitations, which are proton-neutron, neutron-proton reactions, is not limited to examining properties such as Gamow-Teller (GT) resonance energy, the Ikeda sum rule, and cross-section.

Therefore, the determination of nuclear matrix elements of both ground state and excited states and calculation of half-life times is of great importance.

Numerical calculation results of matrix elements of the Pauli spin operator, the orbital angular momentum operator, and the total angular momentum operator obtained as a result of analytical calculations were obtained using FORTRAN 77 programming language. The relativistic β moment matrix elements play an important role in the calculation of the transition probability. Obtaining the transition probability correctly will make a great contribution to the correct interpretation of the *ft* value. For $\lambda^{\pi}=1^{-}$ excited states, the effective interaction strength parameter is used as $\chi_{rank1}=55A^{-5/3}MeVfm^{-2}$.

In this study, rank 1 first-forbidden (FF) beta decay processes for the considered isotopes were investigated by using the proton-neutron quasi-particle random phase approximation (pn-QRPA) in the Schematic Model. For the first-forbidden transitions, the Woods-Saxon (WS) potential is considered as the average field potential in the numerical calculations and the Chepurnov parameterization is taken into account in the selection of the parameters. The pair correlation function constants between nucleons assumed to be $C_n=C_p=12/\sqrt{A}$ and no extinction factor was used to match the experimental results.

The relativistic matrix element of the first-forbidden beta transition operator $\lambda^{\pi}=1^{-}$ is calculated directly analytically without making any assumptions. The problem is analyzed in more detail by adding the potential arising from the spin-orbit interaction in obtaining the matrix elements of the rank 1 first-forbidden beta transition operators. The ξ-approximation was taken into account in the calculation of nuclear matrix beta moments.

Nuclei in the 186⩽A⩽202 mass region undergo β^{-} decay or electron capture (EC) reaction due to the excess number of neutrons. Transition diagrams of some isotopes that make the $0^{+}\leftrightarrow 1^{-}$ transition is shown in Figures 5.1 - 5.8. The value of I (%) indicates the abundance ratio, and the experimental log*ft* values corresponding to this

abundance value are expressed with proton-neutron quasi-particle random phase approximation (pn-QRPA) Woods-Saxon values.

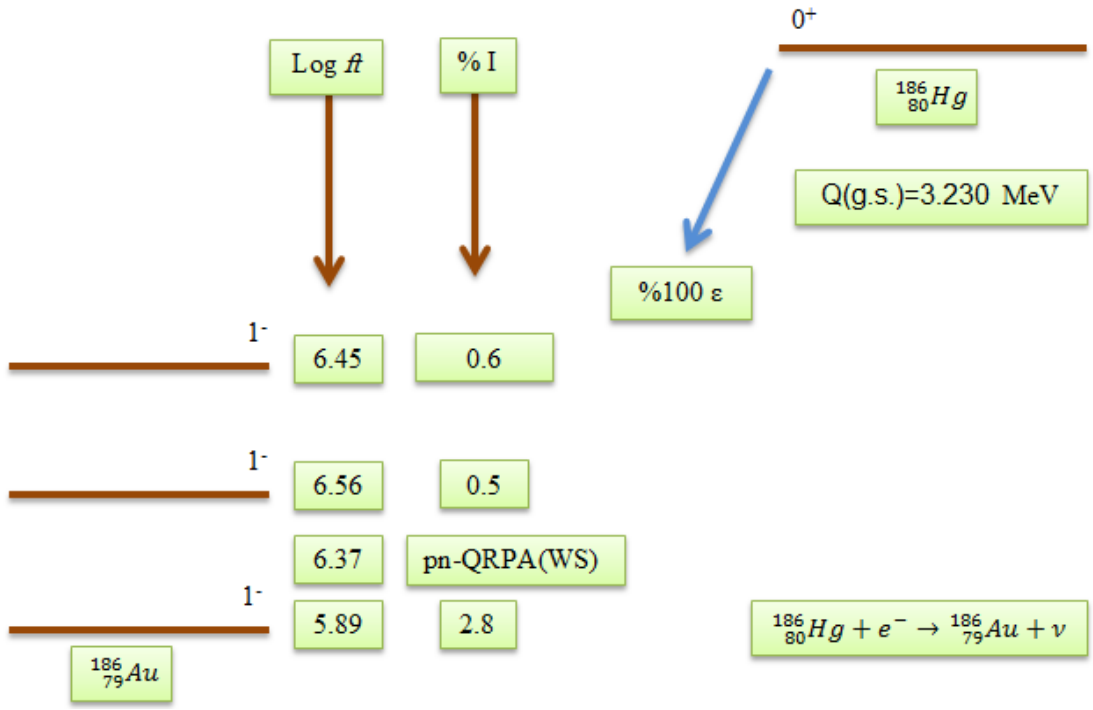

Figure 5.1. Electron capture (ε) transitions diagram of the Hg-186 isotope.

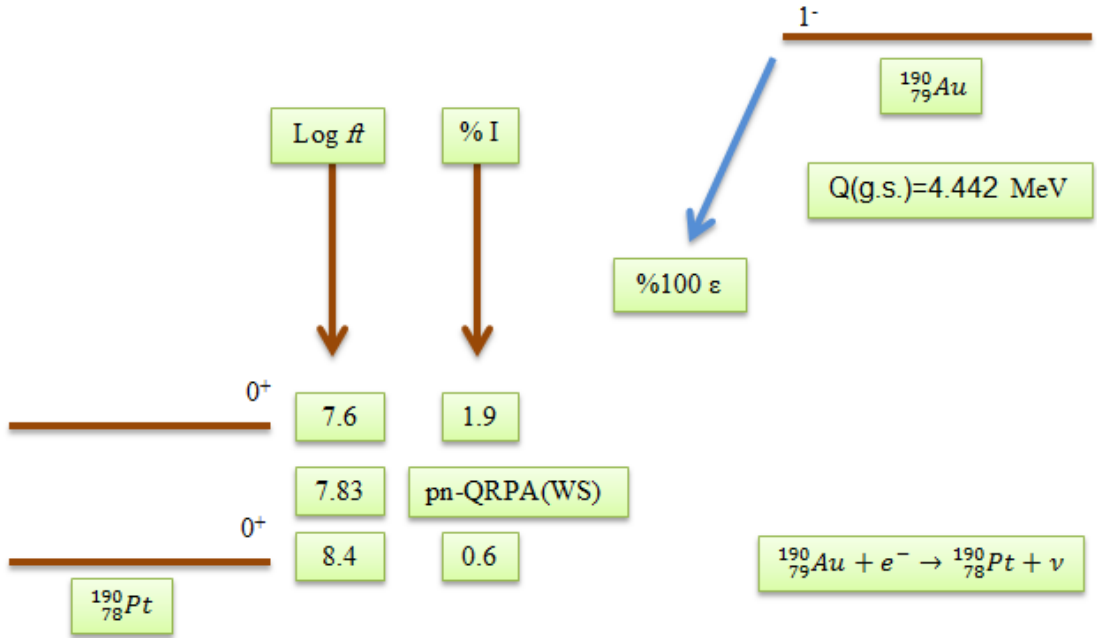

Figure 5.2. Electron capture (ε) transition diagram of the Au-190 isotope.

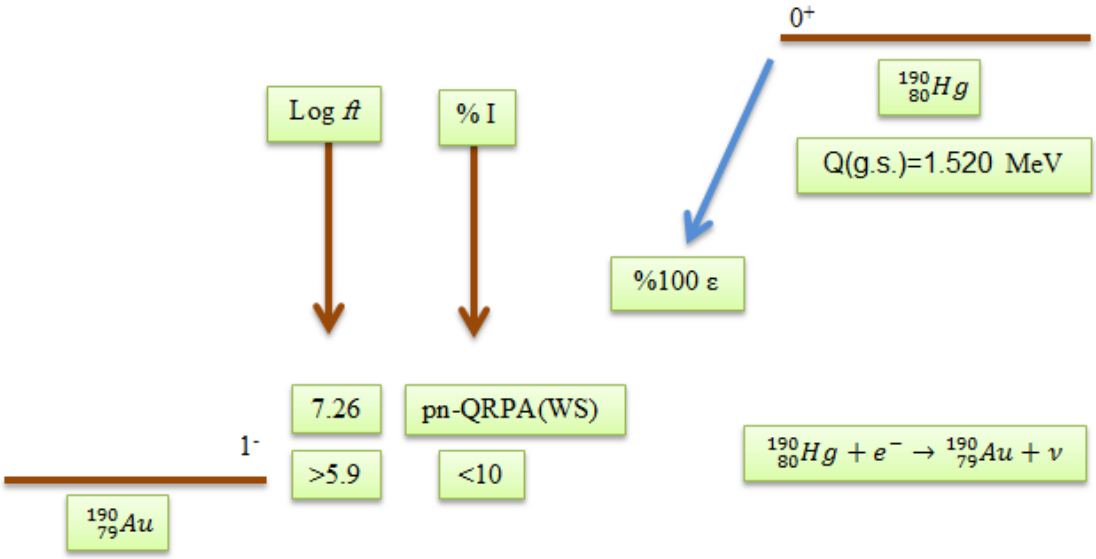

Figure 5.3. Electron capture (ε) transition diagram of the Hg-190 isotope.

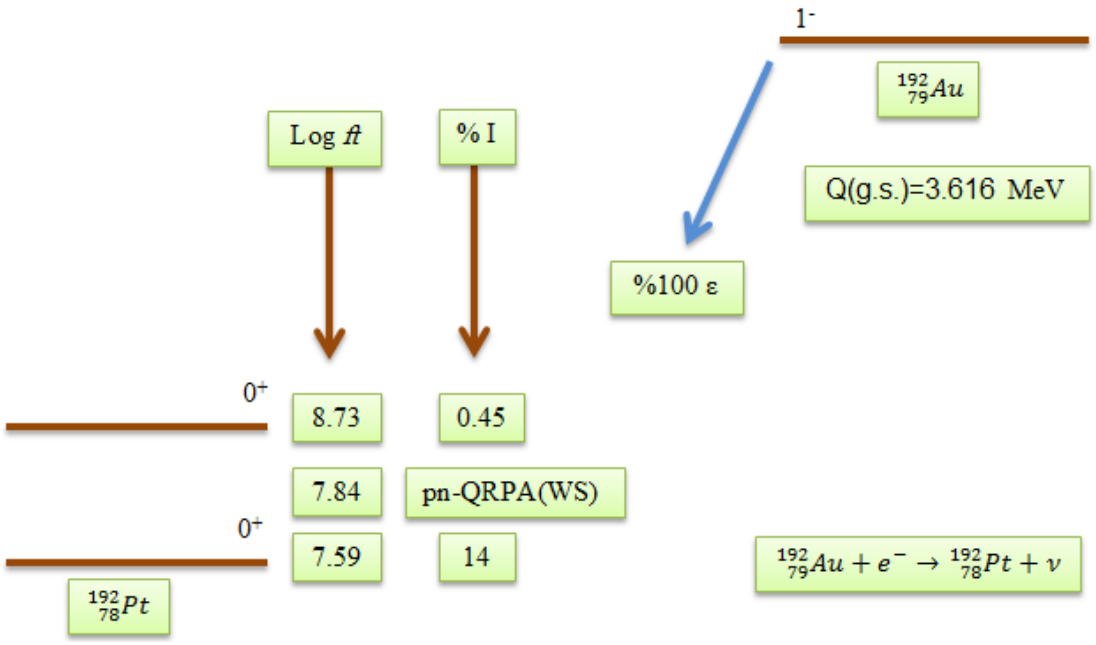

Figure 5.4. Electron capture (ε) transition diagram of the Au-192 isotope.

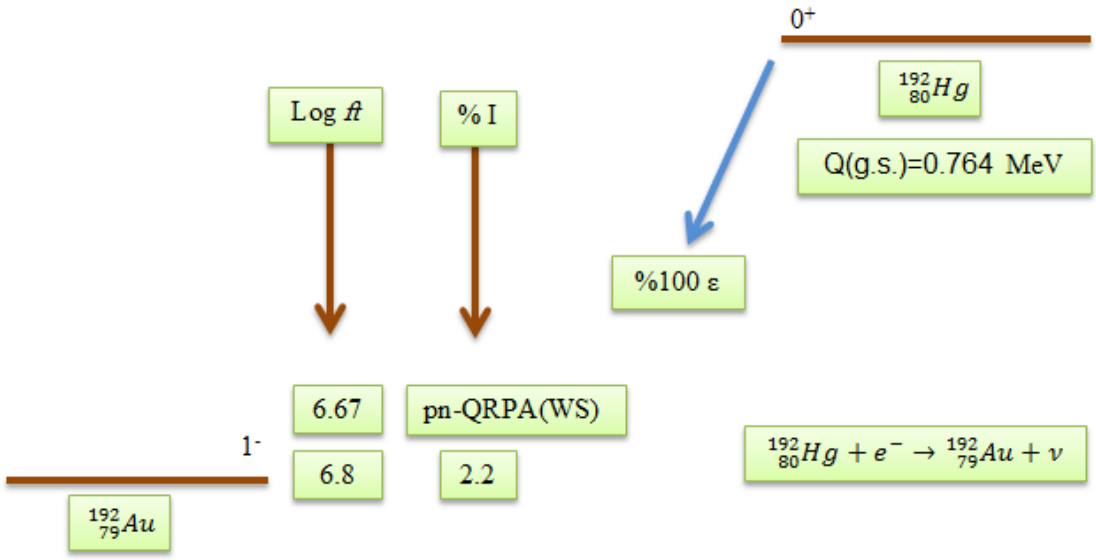

Figure 5.5. Electron capture (ε) transition diagram of the Hg-192 isotope.

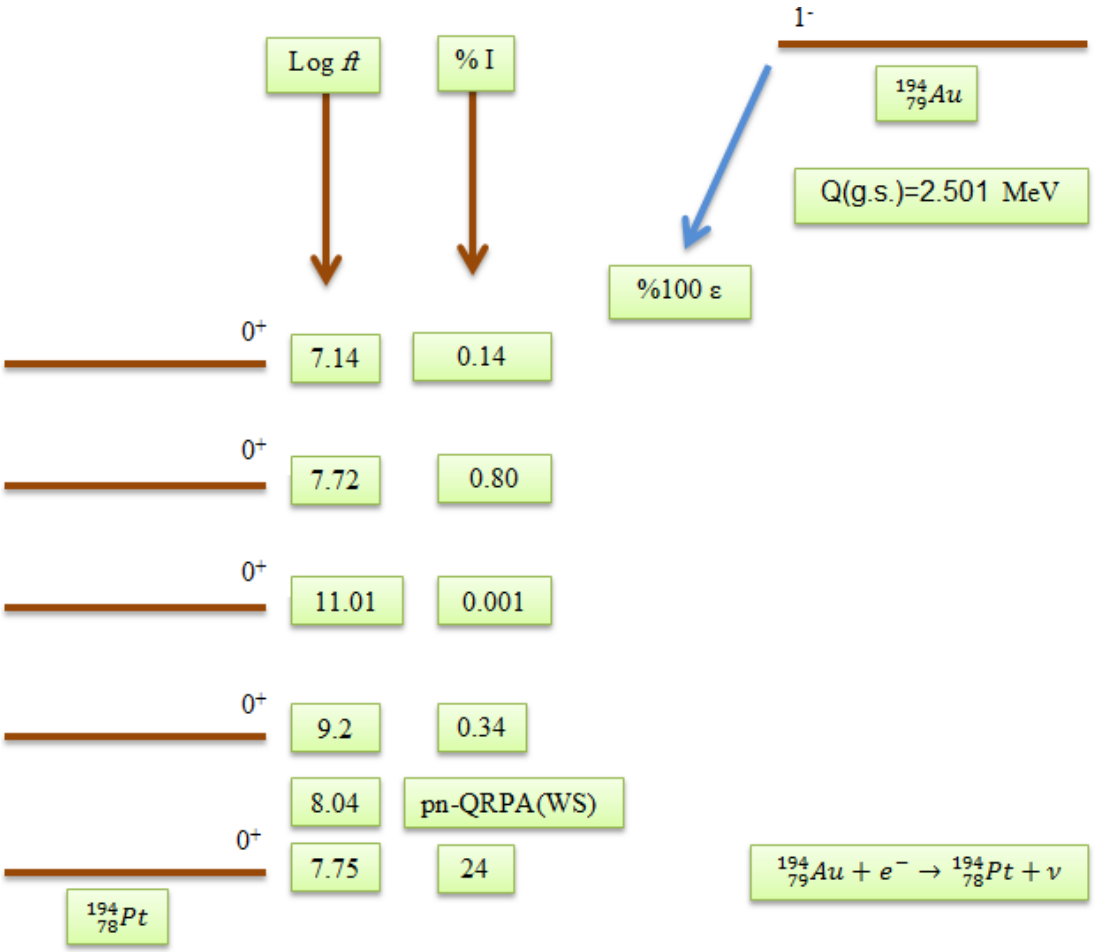

Figure 5.6. Electron capture (ε) transitions diagram of the Au-194 isotope.

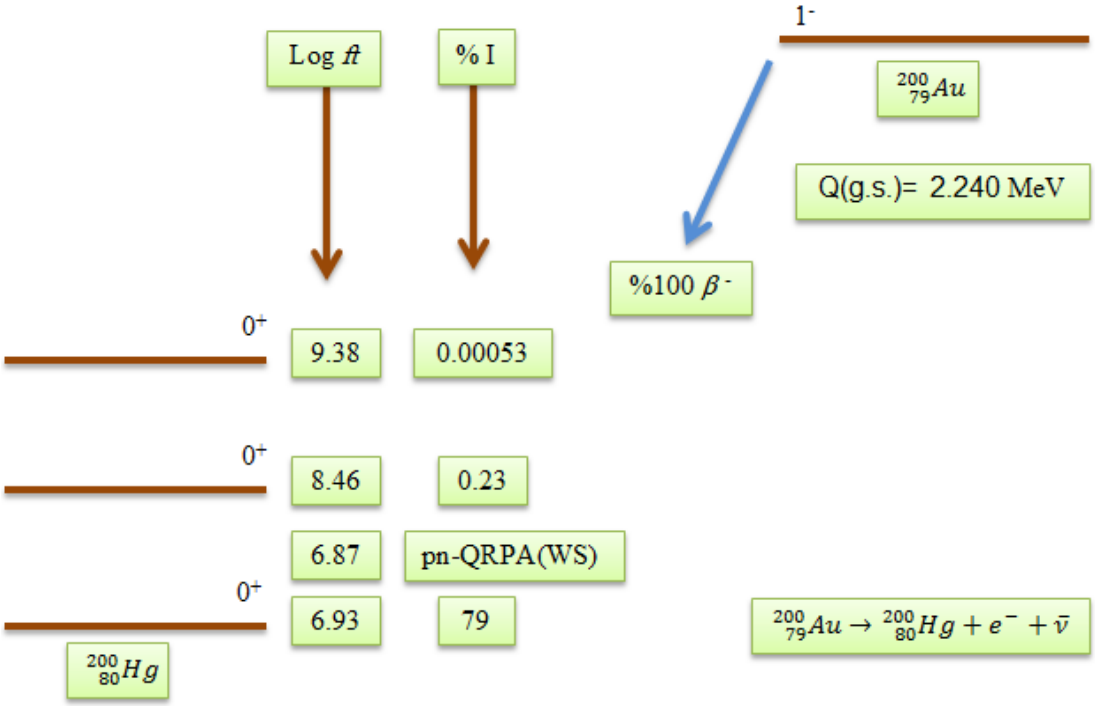

Figure 5.7. Negative beta (β^-) transitions diagram of the Au-200 isotope.

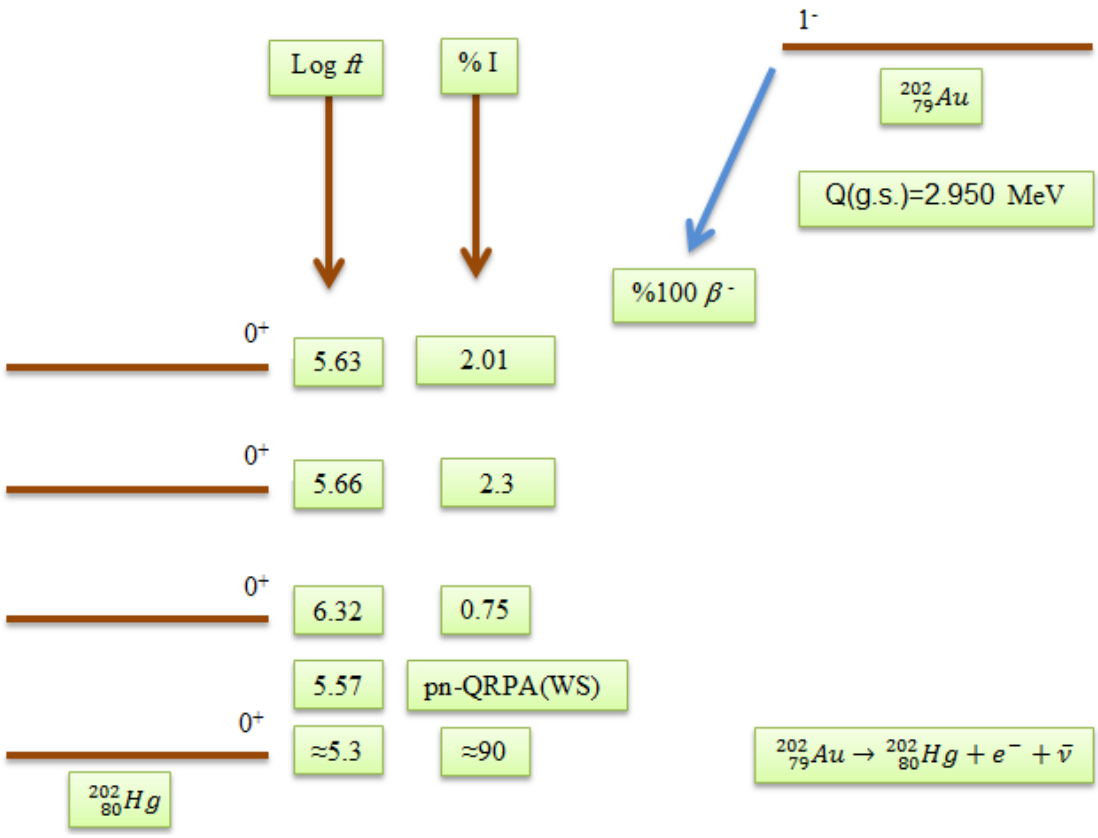

Figure 5.8. Negative beta (β^-) transitions diagram of the Au-202 isotope.

The proton-neutron quasi-particle random phase approximation (pn-QRPA) log*ft* values for isotopes making the first-forbidden $0^+ \rightarrow 1^-$ and $1^- \rightarrow 0^+$ transitions were compared with appropriate experimental values and the results are given in Tables 5.1 – 5.8. The energy values of ω_i (MeV) are the ground state energies of the neighbouring nucleus corresponding to the log*ft* values calculated with the pn-QRPA (WS). As can be seen from all tables, the log*ft* values calculated by the pn-QRPA(WS) method are closer to the experimental values.

Table 5.1. The FF-decay log*ft* for Hg-186 isotope.

Transitions	Experimental [41]			Theoretical	
	ω (MeV)	I (%)	log*ft*	ω (MeV)	log*ft*
$^{186}_{80}Hg(0^+, g.s.) \rightarrow {}^{186}_{79}Au(1^-)$	1.139 4.052 4.642	2.8 0.5 0.6	5.89 6.56 6.45	2.361	6.37

Table 5.2. The FF-decay log*ft* for Au-190 isotope.

Transitions	Experimental [42]			Theoretical	
	ω (MeV)	I (%)	log*ft*	ω (MeV)	log*ft*
$^{190}_{79}Au(1^-, g.s.) \rightarrow {}^{190}_{78}Pt(0^+)$	0.0 0.920	0.6 1.9	8.4 7.6	1.532	7.83

Table 5.3. The FF-decay log*ft* for Hg-190 isotope.

Transitions	Experimental [42]			Theoretical	
	ω (MeV)	I (%)	log*ft*	ω (MeV)	log*ft*
$^{190}_{80}Hg(0^+, g.s.) \rightarrow {}^{190}_{79}Au(1^-)$	0.0	<10	>5.9	0.853	7.26

Table 5.4. The FF-decay log*ft* for Au-192 isotope.

Transitions	Experimental [43]			Theoretical	
	ω (MeV)	I (%)	log*ft*	ω (MeV)	log*ft*
$^{192}_{79}Au(1^-, g.s.) \rightarrow {}^{192}_{78}Pt(0^+)$	0.0 1.195	14 0.45	7.59 8.73	0.765	7.84

Table 5.5. The FF-decay log*ft* for Hg-192 isotope.

Transitions	Experimental [43]			Theoretical	
	ω (MeV)	I (%)	log*ft*	ω (MeV)	log*ft*
$^{192}_{80}Hg(0^+, g.s.) \rightarrow {}^{192}_{79}Au(1^-)$	1.674	2.2	6.8	1.156	6.67

Table 5.6. The FF-decay log*ft* for Au-194 isotope.

Transitions	Experimental [44]			Theoretical	
	ω (MeV)	I (%)	log*ft*	ω (MeV)	log*ft*
$^{194}_{79}Au(1^-, g.s.) \rightarrow {}^{194}_{78}Pt(0^+)$	0.0 1.267 1.893 2.085 2.356	24 0.34 0.001 0.80 0.14	7.95 9.2 11.01 7.72 7.14	1.032	8.04

Table 5.7. The FF-decay log*ft* for Au-200 isotope.

Transitions	Experimental [45]			Theoretical	
	ω (MeV)	I (%)	log*ft*	ω (MeV)	log*ft*
$^{200}_{79}Au(1^-, g.s.) \rightarrow {}^{200}_{80}Hg(0^+)$	0.0 1.029 1.856	79 0.23 0.00053	6.93 8.46 9.38	0.354	6.87

Table 5.8. The FF-decay log*ft* for Au-202 isotope.

Transitions	Experimental [46]			Theoretical	
	ω (MeV)	I (%)	log*ft*	ω (MeV)	log*ft*
$^{202}_{79}Au(1^-, g.s.) \rightarrow {}^{202}_{80}Hg(0^+)$	0.0	≈90	≈5.3	0.902	5.57
	1.411	0.75	6.32		
	1.564	2.3	5.66		
	1.643	2.01	5.63		

PART 6

CONCLUSION

This thesis is of great importance in terms of considering first-forbidden (FF) beta transitions with the WS potential by using the pn-QRPA in the SM. We can summarize the results of the thesis study as follows:

- The first-forbidden (FF) beta transition momentum of the relativistic beta transition operator is directly calculated without any assumptions and the contribution of the spin-orbit term in the shell model potential is neglected in the relativistic calculation of the first-forbidden (FF) beta decay matrix element.

- The results get in better agreement with experimental data as the neutron number increases. It is also expected to give reliable results for nuclei close to the neutron-drip line is available

- Since the charge and mass distribution in the nucleus is closer to the Woods-Saxon (WS) potential function in electron and proton scattering, the base functions of the Woods-Saxon (WS) potential as a potential well in the microscopic model considered,

- The reason for this is that the effective interaction with charge changing between nucleons is considered only in the particle-hole (ph) channel in the aforementioned calculations. The interaction in the particle-particle (pp) channel is very important for a better understanding of the weak interaction theory. We are currently working on FF calculation by using pn-QRPA with the pp channel in Schematic method and this would be treated as a future assignment.

REFERENCES

1. Selam, C., "First forbidden beta transitions of ½ + ↔ ½ - states for Δ J = 0 in spherical odd mass nuclei", ***ALKU Journal Of Science***, (NSP 2018): 174–182 (2019).

2. Evans, H. D., "An absorption comparison of the β-particle spectra of ^{207}ACc (allowed), ^{210}RaE (second forbidden), and 3.5 yr. ^{204}T1 (third forbidden)", ***Proceedings Of The Physical Society. A***, 63 (6): 575–584 (1950).

3. Surman, R., Mumpower, M., Cass, J., Bentley, I., Aprahamian, A., and McLaughlin, G. C., "Sensitivity studies for r-process nucleosynthesis in three astrophysical scenarios", ***EPJ Web Of Conferences***, 66 (07024): (2014).

4. Morales, A.I., Benlliure, J., Kurtukián-Nieto, T., Schmidt, K.H., Verma, S., Regan, P.H., Podolyak, Z., Górska, M., Pietri, S., Kumar, R., and Casarejos, E., "Half-life systematics across the N= 126 shell closure: Role of first-forbidden transitions in the β decay of heavy neutron-rich nuclei", ***Physical Review Letters***, 113(2): 1–5 (2014).

5. Pfeiffer, B., Kratz, K. L., Thielemann, F. K., and Walters, W. B., "Nuclear structure studies for the astrophysical r-process", ***Nuclear Physics A***, 693 (1–2): 282–324 (2001).

6. Dillmann, I., Kratz, K. L., Wöhr, A., Arndt, O., Brown, B. A., Hoff, P., Hjorth-Jensen, M., Köster, U., Ostrowski, A. N., Pfeiffer, B., Seweryniak, D., Shergur, J., and Walters, W. B.,"N=82 Shell quenching of the classical r-process waiting-point nucleus ^{130}Cd", ***Physical Review Letters***, 91 (16): 130–133 (2003).

7. McLaughlin, G. C., and Fuller, G. M., "Weak charge-changing flow in expanding r-process environments", ***The Astrophysical Journal***, 489 (2): 766–771 (1997).

8. Suhonen, J., "Calculation of allowed and first-forbidden beta-decay transitions of odd-odd nuclei", ***Nuclear Physics, Section A***, 563 (2): 205–224 (1993).

9. Nabi, J. U., Çakmak, N., Majid, M., and Selam, C., "Unique first-forbidden β-decay transitions in odd–odd and even–even heavy nuclei", ***Nuclear Physics A***, 957: 1–21 (2017).

10. Sakai, K., "The decay of a new 18.7 h isomer of ^{200}Au", ***Nuclear Physics A***, 118: 361–368 (1968).

11. Halbleib, J. A., "Gamow-Teller beta decay in heavy spherical nuclei and the unlike particle-hole RPA", ***Nuclear Physics A***, 98: 542–568 (1967).

12. Civitarese, O., Krmpotic, F., and Rosso, O. A., "Collective effects included by charge-exchange vibrational modes on $0^- \rightarrow 0^+$ and $2^- \rightarrow 0^+$ first forbidden β-decay transitions", ***Nuclear Physics A***, 453: 45–57 (1986).

13. Kenar, I., Selam, C., and Küçükbursa, A., "$0^- \rightarrow 0^+$ First forbidden β-decay matrix elements in spherical nuclei", ***Mathematical And Computational Applications***, 10 (2): 179–184 (2005).

14. Kenar, ˙I., Ünlü, S., and Maraş, I., "The study of the dependence of radial parts of $0^- \rightarrow 0^+$ first forbidden β-decay matrix elements on the parameters in Woods-Saxon potential", ***Mathematical And Computational Applications***, 13 (1): 1–8 (2008).

15. Cakmak, N., Manisa, K., Unlu, S., and Salam, C., "The investigation of $0^- \leftrightarrow 0^+$ β- decay in some spherical nuclei", ***Pramana-Journal of Physics***, 74 (4): 541-553 (2010).

16. Kotani, T., "Deviation from the ξ approximation in first forbidden β-decay", ***Physical Review***, 114 (3): 795–806 (1959).

17. Bohr, A. A., and Mottelson, B. R., "Beta interaction, single-particle motion", Nuclear Structure, ***W. A. Benjamin INC***, New York, Amsterdam, 395–444 (1969).

18. Nabi, J. U., Çakmak, N., Ullah, A., and Khan, A. U., "β-decay of N= 126 isotones for the r-process nucleosynthesis", ***Physica Scripta***, 96 (11): 1-18 (2021).

19. Nabi, J. U., Cakmak, N., Stoica, S., and Iftikhar, Z., "First-forbidden transitions and stellar β-decay rates of Zn and Ge isotopes", ***Physica Scripta***, 90 (11): 1-12 (2015).

20. Nabi, J. U., Çakmak, N., and Iftikhar, Z., "First-forbidden β-decay rates, energy rates of β-delayed neutrons and probability of β-delayed neutron emissions for neutron-rich nickel isotopes", ***European Physical Journal A***, 52 (1): 1–14 (2016).

21. Cakmak, N., Cakmak, S., Selam, C., and Unlu, S., "Dipole and spin-dipole strength distributions in ^{124,126,128,130}Te isotopes", ***Pramana***, 90 (2), 1-7 (2018).

22. Ullah, A., Riaz, M., Nabi, J. U., Böyükata, M., and Çakmak, N., "Effect of deformation on Gamow-teller strength and electron capture cross-section for isotopes of chromium", ***Bitlis Eren University Journal of Science and Technology***, 10(1): 25-29 (2020).

23. Çakmak, Ş., and Çakmak, N., "Beta decay log*ft* values for zinc isotopes by using pn-QRPA", ***Nuclear Physics A***, 1015 (12): 1-16 (2021).

24. Wilson, F. L., "Fermi's theory of beta decay", ***American Journal Of Physics***, 36 (12): 45–57 (1968).

25. Langanke, K., and Martínez-Pinedo, G., "Nuclear weak-interaction processes in stars", ***Reviews Of Modern Physics***, 75 (3): 819–862 (2003).

26. Krane, K. S., "Beta decay", Introductory nuclear physics, ***John Wiley Sons INC***, United States Of America, 271–292 (1988).

27. Greiner, W., and Maruhn, J. A., "Nuclear models", ***Springer***, Berlin, Almanya, 237–245 (1996).

28. Suhonen, J., and Civitarese, O., "Weak-interaction and nuclear structure aspects of nuclear double beta decay", ***Physics Reports***, 300: 123-214 (1998).

29. Vergados, J. D., "The neutrinoless double beta decay from a modern perspective", ***Physics Report***, 361 (1): 1–56 (2002).

30. Kortelainen, M., and Suhonen, J., "Microscopic study of muon-capture transitions in nuclei involved in doubled-beta-decay processes", ***Nuclear Physics A***, 713 (3–4): 501–521 (2003).

31. Suhonen, J., "From nucleons to nucleus: Concepts of microscopic nuclear theory", ***Springer***, Berlin Heidelberg, Finland, 158–163 (2007).

32. Internet: İnternet: Nükleer Enerji Dünyası, "Radyasyon Türleri", **http://www.nukleer.web.tr/temel_konular/radyasyonturleri.html**.

33. Lee, T. D., and Yang, C. N., "Question of parity conservation in weak interactions", ***Physical Review***, 104 (1): 254–158 (1956).

34. Arya, A. P., "Beta bozunumu", Çekirdek Fiziğinin Esasları, Yusuf Şahin, ***Aktif Yayın Dağıtım***, Erzurum, 334 (1999).

35. Hartwing, G., and Schopper, H., "β-γ Circular polarization correlation of ^{124}Sb", ***Physical Review Journals***, 4 (6): 293–295 (1960).

36. Porter, F. T., and Day, P. P., "0^- to 0^+ transition ^{144}Pr → ^{144}Nd", ***Physical Review Journals***, 114 (5): 1286–1296 (1959).

37. Çakmak, N., "Tek çekirdeklerde yük değişimli etkileşmelerinin Pyatov yöntemi ile incelenmesi", ***Anadolu Üniversitesi Fen Bilimleri Enstitüsü***, Eskişehir, 20-23 (2008).

38. Varshalovich, D. A., Moskalev, A. N., and Khersonsskii, V. K., "Matrix elements of irreducible tensor operators", Quantum theory of angular momentum, ***Word Scientific***, Singapur, New Jersey, Hongkong, 475–504

(1988).

39. Suhonen, J., "From nucleons to nucleus: Concepts of microscopic nuclear theory", ***Springer***, Berlin Heidelberg, Finland, 595–611 (2007).

40. Toivanen, J., and Suhonen, J., "Renormalized proton-neutron quasi-particle random-phase approximation and its application to double beta decay", ***Physical review letters***, 75 (3): 410-413 (1995).

41. Baglin, C. M., "Nuclear data sheets for A= 186", ***Nuclear Data Sheets***, 99 (1): 1-196 (2003).

42. Singh, B., "Nuclear data sheets for A= 190", ***Nuclear Data Sheets***, 99(2): 275-481 (2003).

43. Baglin, C. M., "Nuclear data sheets for A= 192", ***Nuclear Data Sheets***, 113 (8-9): 1871-2111 (2012).

44. Singh, B., "Nuclear data sheets for A= 194", ***Nuclear Data Sheets***, 107(6): 1531-1746 (2006).

45. Kondev, F. G., & Lalkovski, S., "Nuclear data sheets for A= 200", ***Nuclear Data Sheets***, 108(7): 1471-1582 (2007).

46. Zhu, S., & Kondev, F. G., "Nuclear Data Sheets for A= 202", ***Nuclear Data Sheets***, 109(3): 699-786 (2008).

RESUME

Mohammed Hawez Saber Saber completed high school education at Kurdistan High School in Erbil/Iraq. He obtained a bachelor's degree from the Department of Physics in the College of the Science/University of Duhok in 2012. He moved to Karabuk/Turkey for the Master of Science Education and started his master education at the Department of Physics / Karabuk University in 2019.